Responsive and Post-functionalizable Polymeric Microspheres

Rafael Eduardo Paiva Feener[a]

[a]   Master in Nanoscience and Molecular Nanotechnology, Universidad de La Laguna
   alu0100893953@ull.edu.es

Abstract: Insertion of reversible covalent bonds in polymeric frameworks allows to modify their properties and may provide a responsive material. Such dynamic polymers take advantage of the ability of dynamic covalent reactions to reach thermodynamic equilibrium, and therefore they can adapt to changing chemical environments. Nucleophilic aromatic substitution of tetrazines (S_NTz), a novel dynamic covalent reaction, has been used to synthesize brand-new dynamic polymer networks. This reaction combines the advantages of its reversible nature with the chemical versatility of the tetrazine ring (Tz). In fact, the latter makes it possible to easily attach molecular fragments by inverse electron demand Diels-Alder reaction (IEDDA).

In this work, uniform microspheres have been easily obtained in homogeneous phase. They can be easily depolymerized by the right chemical stimulus enabling and efficient recycling. Monomeric exchange also allowed converting one polymer into another (metamorphosis). Finally, these networks could be post-functionalized by IEDDA reaction, which modulates the physico-chemical properties of the material (e.g., solubility in water), but also locks the exchange. For all the above, tetrazine dynamic polymers are envisioned as a quite promising and versatile kind of materials.

Introduction

Dynamic covalent chemistry (DCC) involves a group of reversible reactions constantly reaching to thermodynamic equilibrium, [1-4] which confers them the ability to amend structural "mistakes" and to easily adapt to changing environments. The addition of this kind of reversible covalent bonds to polymeric structures, usually thought as hard-to-change or immovable, opens a window of possibility allowing them to become responsive, adaptable, and even recyclable. [5-12] This has already been well performed via imine formation, [13-15] esterification of boronic acids, [16-17] Diels-Alder cycloadditions, [18-20] and other reversible processes, [21-28] giving rise to smart materials based on dynamic covalent polymers, adaptable networks suitable to shift their shape or change their network topology upon the application of the right stimulus.

Recently our group discovered the nucleophilic aromatic substitution of tetrazines (S_NTz), a novel covalent dynamic reaction, which not only benefits from its reversibility, but also from the different properties displayed by tetrazine rings.[29] Such reaction quickly exchanges alkylthiols and phenols in positions 3 and 6 at room conditions (Figure1a). Also, this exchange will be finished if one of the reagents is a much better leaving group than the other. It is remarkable that this reaction can be carried out in aqueous environments, but most importantly, all of these can be functionalized by Inverse Electron Demand Diels-Alder (IEDDA) reaction, which cancels the exchange (Figure 1b). Therefore, molecular fragments may be attached to the
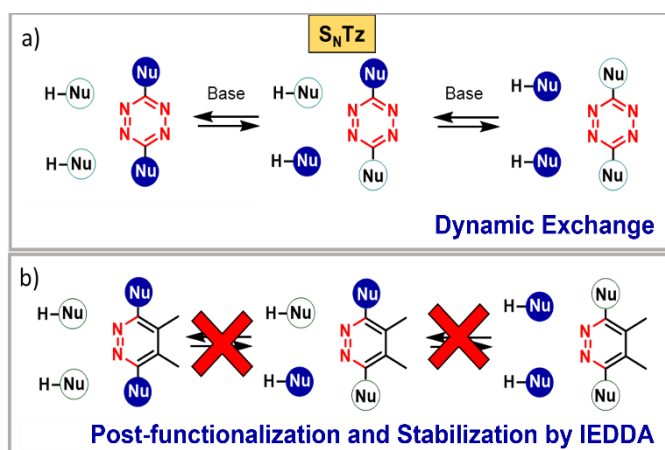
Figure 1. Synthesis of polymers by Nucleophilic Tetrazine Substitution (S_NTz) benefits from a) its dynamic behavior; b) post-functionalization by inverse electron demand Diels-Alder reaction (IEDDA) which also stabilizes the structure by locking the exchange

backbone of the polymers, conferring post-stabilization to the network.

As it was abovementioned, covalent dynamics applied to materials science is useful to obtain materials with interesting properties, therefore, it is logical to think that a polymeric compound obtained through S_NTz would benefit from both reversibility of chemical bonds, and the important features imparted given by the tetrazine ring. This could lead to the obtention of a novel kind of promising dynamic covalent polymers. Herein we report an efficient polymerization method through the click-like reaction S_NTz. The polymers have been obtained mainly as uniform microspheres that take advantage both from dynamic behaviour and tetrazine rings together (Figure 1). Thus, they respond to chemical stimuli

and can be depolymerized and recycled easily; [30-31] additionally they can be post-functionalized which stabilizes the structure against degradation.

Methodology and Results

All the polymers included in this work were easily synthesized at room temperature in high yield by $S_N Tz$. The corresponding polyphenol or thiol were mixed in acetonitrile with 3,6-dichloro-1,2,4,5-tetrazine (0.5 equivalents per OH/SH) and triethylamine (TEA) (Figure 2).[32] After a few seconds a coloured solid clearly precipitated out of the solution. Then filtration of such precipitate, followed by washings with acetonitrile, water and methanol, and finally drying under vacuum, gave a very good yield of polymers (70-96%). Yields decrease in other solvents or with different molar ratios. [32] All the materials synthesized were virtually insoluble in any solvent tested (hexane, acetonitrile, methanol, acetone, dichloromethane, dimethylformamide, dimethylsulfoxide and water).
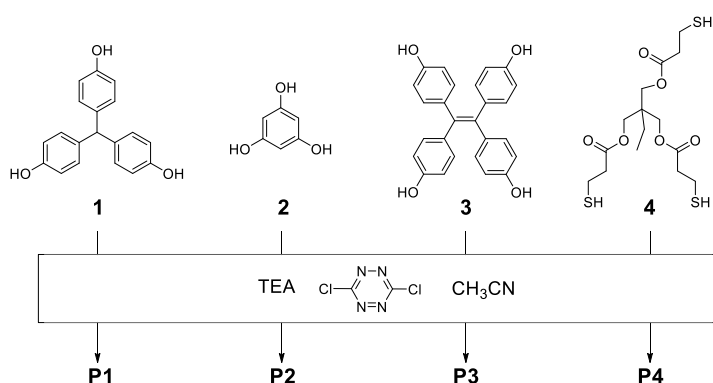
Figure 2. Synthesis of the tetrazine polymer networks.

In the IR spectra of the polymers, the peaks corresponding to the OH and SH bonds disappeared, meaning a high conversion degree of the starting materials, which is consisting with the results obtained by elemental analysis. Stability at high temperatures was determined by TGA analysis, through the temperature at which the polymers lose 5% of their weight (T_D). **P1** remain stable at temperatures up to 294°C, being **P3** and **P4** slightly less stable, while **P2** shows the lowest thermal stability (T_D=192°C). It is worth mentioning that **P3** is not fluorescent even when rotational restriction of tetraphenylethene is known to induce fluorescence.[33] That is probably explained by the quenching effect of the electron poor tetrazine on the tetraphenylethene moiety. X-ray diffraction indicates that none of them possess a crystalline structure, being this common in polymeric compounds.

Nevertheless, scanning electron microscopy (SEM) shows that **P1**, **P2**, and **P3** exhibit spherical shape and that **P4**, the thiol polymer, happened to be amorphous (Figure 3). Polymer **P1** is the most homogeneous, presenting an average diameter of 1.05±0.04 μm, however, this value, as well as yield, could easily be modified by changing the temperature, concentration or solvent employed. [36] For the other phenolic compounds, dispersion was less regular, and, in general, the spheres were smaller.
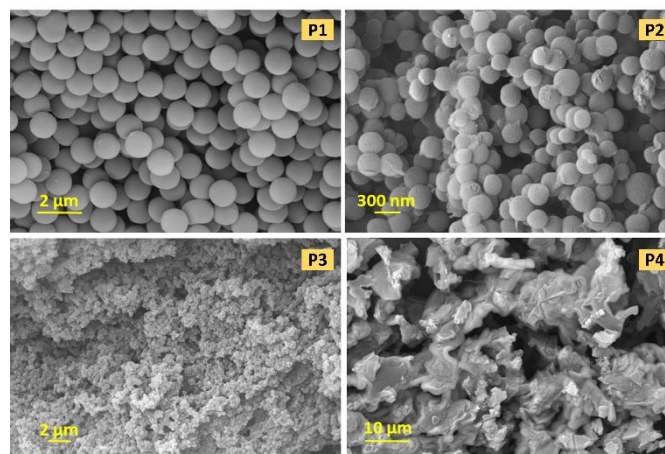


Figure 3. SEM images of the polymers.

It is known that alkyl thiols can easily substitute phenols in a tetrazine ring. [29] Therefore, addition of thiols to the polymers could be a way of depolymeryzation. In fact, degradation of **P1** was quickly carried out in the presence of triethylamine and dodecanethiol **5**, yielding a 99% recovery of the original monomer **1**. Figure 4 shows the stacked NMR spectra in which we can clearly observe such degradation. For the rest of polyphenol polymers similar results were obtained. If an acidic thiol is used, base is not required. For example, hydrogen sulphide (pKa= 6.9) could degrade **P1** by itself in water. It is worth recalling that, in some kinds of cancer, tumoral cells bear a high concentration of H_2S. [34] Therefore, tetrazine dynamic polymers may be designed for applications in stimuli-induced drug release or in theragnostics. Other good nucleophiles, such us fluoride, are also able to depolymerize **P1** in methanol.

According to what was stated, chemical degradation occurs in presence of a better nucleophile, e.g., alkyl thiols, however, in the case of branched substituents, the results can vary drastically. Reaction with a polythiol such as **4** predictably would lead to a

monomeric exchange, yielding a polymer different from the initial one.
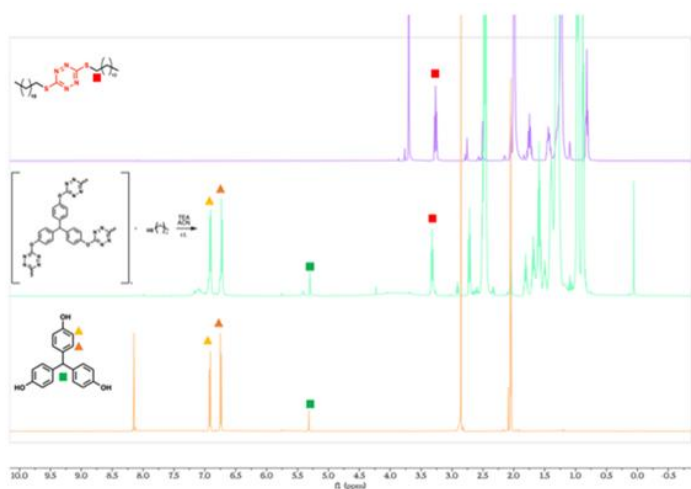
Figure 4. Chemically induced recycling of the monomer. Stacked NMR spectra of the monomer 1 (bottom), the dodecanethiol tetrazine dimer (top) and the crude of the recycling reaction in CD3CN after 3h.
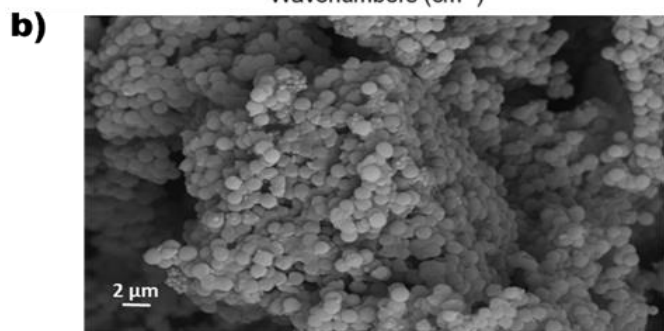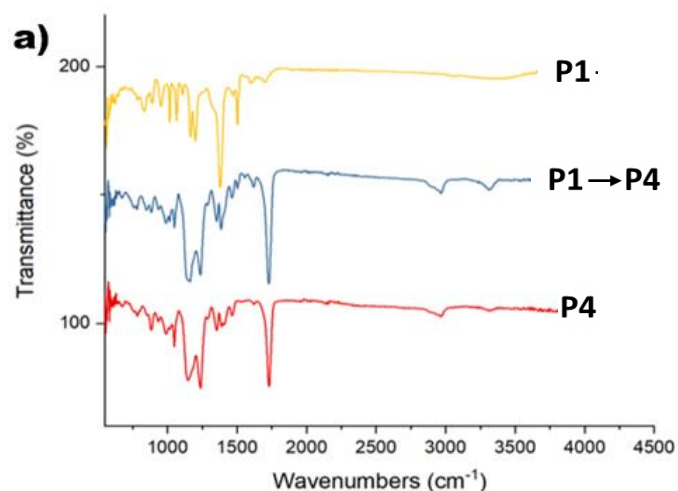
Figure 5. a) Stacked IR of **P1** (blue), metamorphosis from **P1** to **P4** (red) and **P4** (black). It is clearly seen that the latter two are identical; b) SEM image of the metamorphosed polymer.

This was successfully proved by adding **4** and TEA to a suspension of **P1** in acetonitrile. Triphenol **1** was released along with the apparition of polymer **P4**. This metamorphosis can easily be confirmed by the IR spectra (Figure 5a). Clearly, the composition of both metamorphosed and directly obtained **P4** are identical. Nevertheless, it is quite interesting that, after the monomeric exchange, **P1**'s spherical morphology prevailed (Figure 5b), even when **P4** made directly from **4** had a totally different shape (Figure 3). A possible explanation might be a template effect of **P1**'s microspheres during the exchange.

Traditionally, the modulation of the properties of a polymeric compound is made through designing and modifying monomers in advance. In contrast, thanks to the tetrazine rings included in their structure, post-functionalization is possible by IEDDA. It is quite an interesting and appealing quality, because post-functionalization allows us to modulate important properties by simply attaching molecular fragments directly to the backbone of our material.
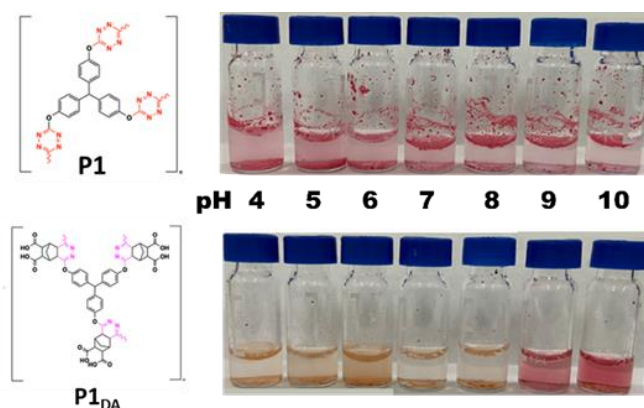
Figure 6. Solubility in water of pristine P1 and post-functionalized P1DA at different pH.

In order to change the solubility of our polymer, a reactive olefin including two polar groups was chosen for IEDDA reaction: cis-5-norbornene-endo-2,3-dicarboxylic acid (**6**). The reaction was performed by heating a suspension of **P1** and **6** in acetonitrile at 80ºC for 72h. A brownish solid, **P1$_{DA}$**, was obtained with 70% yield. Both IR spectra and solid state ^{13}C NMR report major changes and also SEM reveals morphologic variation (microspheres are not preserved). [32] Despite **P1** is completely insoluble in water regardless of the pH, the carboxylate groups covering the surface of **P1$_{DA}$** make it soluble in water at high pH as expected (Figure 6). Furthermore, post-

functionalization increases stabilization in the polymer network, so they cannot be degraded by thiols. In fact, **P1$_{DA}$** was not affected by dodecanethiol and triethylamine, even after 24h.

Conclusions

In conclusion, responsive and post-functionalizable microspheres have been made out of tetrazine dynamic polymer networks. These kind of polymers have shown a lot of potential in the field of materials science as well as in supramolecular chemistry and biomedicine. Indeed, they benefit from all the advantages of dynamic covalent chemistry while displaying the chemical versatility of the tetrazine ring. These polymers were quickly and efficiently designed and synthesized, in quite simple conditions, thanks to the click-like S_NTz reaction. They underwent controlled depolymerization upon the application of the right stimuli, e.g., chemical reagents such as thiols in basic medium, H_2S in water, or fluoride anions, efficiently recovering the constituent monomers, allowing an effective recycling. Additionally, irreversible interconversion between two different polymers was possible by monomeric exchange (metamorphosis). Furthermore, all tetrazine dynamic polymers are suitable for post-functionalization by IEDDA reaction, making possible the modulation of their properties such as solubility in water, while locking the exchange by boosting their stability. All these remarkable properties make tetrazine dynamic polymer networks an attractive and useful kind of materials which may probably find applicability in the synthesis of porous polymers, recyclable conductive materials, smart filters, controlled release or theragnostics.

Acknowledgements

I would also like to thank the people I have been honored and pleasured to meet during the process of realizing this master's degree, especially the group I have been able to work in. I have learned many things from and along with you, but overall, the long and winding road of research has been much more enjoyable.

References

[1]   S. J. Rowan, S. J. Cantrill, G. R. L. Cousins, J. K. M. Sanders, J. F. Stoddart, *Angew. Chem.* **2002**, *114*, 938–993; *Angew. Chem. Int. Ed.* **2002**, *41*, 898–952.

[2]   *Dynamic Covalent Chemistry: Principles, Reactions, and Applications* (Eds.: W. Zhang, Y. Jin), John Wiley & Sons Ltd, **2018**.

[3]   P. T. Corbett, J. Leclaire, L. Vial, K. R. West, J. L. Wietor, J. K. M. Sanders, S. Otto, *Chem. Rev.* **2006**, *106*, 3652–3711.

[4]   Y. Jin, C. Yu, R. J. Denman, W. Zhang, *Chem. Soc. Rev.* **2013**, *42*, 6634–6654.

[5]   W. Zou, J. Dong, Y. Luo, Q. Zhao, T. Xie, *Adv. Mater.* **2017**, *29*, 1606100.

[6]   S. Billiet, K. De Bruycker, F. Driessen, H. Goossens, V. Van Speybroeck, J. M. Winne, F. E. Du Prez, *Nat. Chem.* **2014**, *6*, 815–821.

[7]   N. Zheng, Y. Xu, Q. Zhao, T. Xie, *Chem. Rev.* **2021**, *121*, 1716–1745.

[8]   J. M. Winne, L. Leibler, F. E. Du Prez, *Polym. Chem.* **2019**, *10*, 6091-6108.

[9]   F. García, M. M. J. Smulders, *J. Polym. Sci., Part A: Polym. Chem.* **2016**, *54*, 3551-3577.

[10] C. J. Kloxin, T. F. Scott, B. J. Adzima, C. N. Bowman, *Macromolecules* **2010**, *43*, 2643–2653.

[11] P. Chakma, D. Konkolewicz, *Angew. Chem.* **2019**, 131, 9784-9797; *Angew. Chem. Int. Ed.* **2019**, *58*, 9682-9695.

[12] M. Podgórski, B. D. Fairbanks, B. E. Kirkpatrick, M. McBride, A. Martínez, A. Dobson, N. J. Bongiardina, C. N. Bowman, *Adv. Mater.* **2020**, *32*, 1906876.

[13] N. Kuhl, S. Bode, R. K. Bose, J. Vitz, A. Seifert, S. Hoeppener, S. J. García, S. Spange, S. van der Zwaag, M. D. Hager, U. S. Schubert, *Adv. Funct. Mat.* **2015**, *25*, 3295-3301.

[14] S. K. Schoustra, J. A. Dijksman, H. Zuilhof, M. M. J. Smulders, *Chem. Sci.* **2021**, *12*, 293-302.

[15] S. K. Schoustra, T. Groeneveld, M. M. J. Smulders, *Polym. Chem.* **2021**, *12*, 1635-1642.

[16] M. Röttger, T. Domenech, R. van der Weegen, A. Breuillac, R. Nicolaÿ, L. Leibler, *Science* **2017**, *356*, 62– 65.

[17] J. J. Cash, T. Kubo, A. P. Bapat, B. S. Sumerlin, *Macromolecules* **2015**, *48*, 2098–2106.

[18] B. J. Adzima, H. A. Aguirre, C. J. Kloxin, T. F. Scott, C. N. Bowman, *Macromolecules* **2008**, *41*, 9112–9117.

[19] X. Chen, M. A. Dam, K. Ono, A. Mal, H. Shen, S. R. Nutt, K. Sheran, F. Wudl, *Science*, **2002**, *295*, 1698-1702.

[20]   K. K. Oehlenschlaeger, J. O. Mueller, J. Brandt, S. Hilf, A. Lederer, M. Wilhelm, R. Graf, M. L. Coote, F. G. Schmidt, C. Barner-Kowollik, *Adv. Mater.* **2014**, *26*, 3561-3566.

[21]   M. Podgórski, S. Mavila, S. Huang, N. Spurgin, J. Sinha, C. N. Bowman, *Angew. Chem.* **2020**, *132*, 9431-9435; *Angew. Chem. Int. Ed.* **2020**, *59*, 9345-9349.

[22]   N. Van Herck, D. Maes, K. Unal, M. Guerre, J. M. Winne, F. E. Du Prez, *Angew. Chem.* **2020**, *132*, 9431-9435; *Angew. Chem. Int. Ed.* **2020**, *59*, 3609-3617.

[23]   K. Jin, L. Li, J. M. Torkelson, *Adv. Mater.* **2016**, *28*, 6746-6750.

[24]   Y. Nishimura, J. Chung, H. Muradyan, Z. Guan, *J. Am. Chem. Soc.* **2017**, *139*, 14881–14884.

[25]   Y.-X. Lu, Z. Guan, *J. Am. Chem. Soc.* **2012**, *134*, 14226– 14231.

[26]   M. Capelot, D. Montarnal, F. Tournilhac, L. Leibler, *J. Am. Chem. Soc.* **2012**, *134*, 7664– 7667.

[27]   M. M. Obadia, B. P. Mudraboyina, A. Serghei, D. Montarnal, E. Drockenmuller, *J. Am. Chem. Soc.* **2015**, *137*, 6078– 6083.

[28]   Y. Zhang, H. Ying, K. R. Hart, Y. Wu, A. J. Hsu, A. M. Coppola, T. A. Kim, K. Yang, N. R. Sottos, S. R. White, J. Cheng, *Adv. Mater.* **2016**, *28*, 7646-7651.

[29]   T. Santos, D. S. Rivero, Y. Pérez-Pérez, E. Martín-Encinas, J. Pasán, A. H. Daranas, R. Carrillo, *Angew. Chem.* **2021**, *133*, 18931-18939; *Angew. Chem. Int. Ed.* **2021**, *60*, 18783-18791.

[30]   D. Sathe, J. Zhou, H. Chen, H.-W. Su, W. Xie, T.-G. Hsu, B. R. Schrage, T. Smith, C. J. Ziegler, J. Wang, *Nat. Chem.* **2021**, *13*, 743–750.

[31]   J.-B. Zhu, E. M. Watson, J. Tang, E. Y.-X. Chen, *Science* **2015**, *360*, 398-403.

[32]   See the Supporting Information.

[33]   Z. Zhao, J. W. Y. Lam, B. Z. Tang, *J. Mater. Chem.* **2012**, *22*, 23726-23740.

[34]   C. Szabo, C. Coletta, C. Chao, K. Módis, B. Szczesny, A. Papapetropoulos, M. R. Hellmich, *Proc. Natl Acad. Sci. USA* **2013**, *110*, 12474-12479.

SUPPORTING INFORMATION

Responsive and Post-functionalizable Polymeric

Microspheres

Rafael E. Paiva-Feener

Master in Nanoscience and Molecular Nanotechnology, Universidad de La Laguna.

Index

1. <u>Materials and methods.</u>

All reagents from commercial suppliers were used without further purification. All solvents were freshly distilled before use from appropriate drying agents. All other reagents were recrystallized or distilled when necessary. Reactions were performed under a dry nitrogen atmosphere. Analytical TLCs were performed with silica gel 60 F$_{254}$ plates. Visualization was accomplished by UV light or vanillin with acetic and sulfuric acid in ethanol with heating. Column chromatography was carried out using silica gel 60 (230-400 mesh ASTM). ^{1}H NMR spectra were recorded at 500 MHz and 400MHz, ^{13}C NMR spectra were recorded at 126 MHz and 100 MHz. Solid state ^{13}C NMR were recorded with a VARIAN INOVA-750. Chemical shifts were reported in units (ppm) by assigning TMS resonance in the ^{1}H NMR spectrum as 0.00 ppm (deuterated chloroform, 7.26 ppm; acetonitrile-d_3 1.94 ppm; DMSO-d_6 2.50 ppm; acetone-d_6 2.05 ppm). Data were reported as follows: chemical shift, multiplicity (s = singlet, d = doublet, t = triplet, q=quartet, dd = double doublet, ddd = double double doublet, m =multiplet and br = broad), coupling constant (J values) in Hz and integration. Chemical shifts for ^{13}C NMR spectra were recorded in ppm from tetramethylsilane using the central peak of CDCl$_3$ (77.14 ppm) as the internal standard. High resolution mass spectra (HRMS) were measured by ESI method with an Agilent LC-Q-TOF-MS 6520 spectrometer. SEM images were recorded with a ZEISS EVO 15 and a ZEISS FESEM ULTRA Plus microscopes. TGA analysis were developed in a DTA-TGA Q600 instrument. IR experiments were done in a Bruker IFS 66/S equipment with an ATR tool for direct solid measurements. All the statistics calculus and graphics were obtained using Origin 2019 and the measurements over the SEM images were developed with an open-source program, ImageJ, with a minimum number of 30 measures for obtaining the results. Specific surface areas were calculated using a BET (multi-point) treatment of N$_2$ adsorption isotherm data generated on a Micromeritics ASAP 2020 porosimeter. Each sample (around 100 mg) was degassed at 60 °C for 5 h and then backfilled with N$_2$. N$_2$ adsorption isotherms were generated by incremental exposure to ultrahigh-purity nitrogen up to 1 atm in a liquid nitrogen (77 K) bath, and surface parameters were determined using BET adsorption models included in the instrument software (Micromeritics ASAP 2020 V4.00).

Size measure protocol: the polymer of interest, in this case P1, was suspended in ACN or ethanol and sonicated. A fraction was taken with a pipette, deposited on the SEM sample holder and the solvent was allowed to evaporate. After obtaining the SEM images, they were opened and treated with the open-source software J-Image. First, the image was thresholded and the size of the particle was obtained with the software. Finally, a distribution of the obtained data was performed on OriginLab.
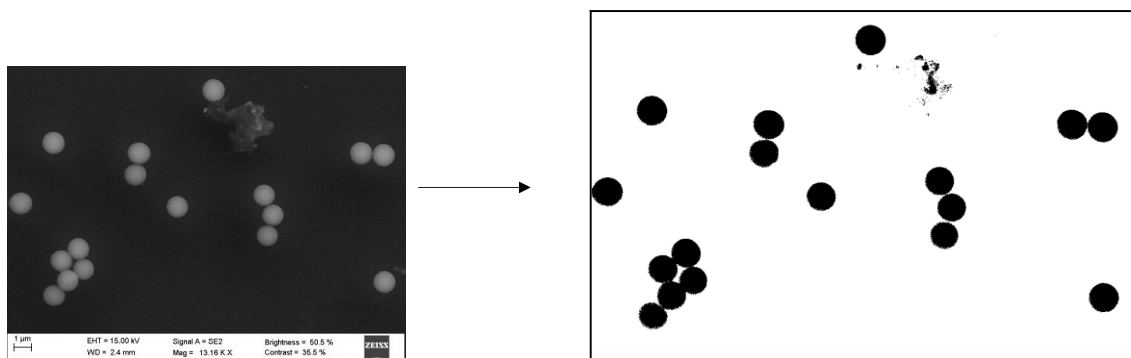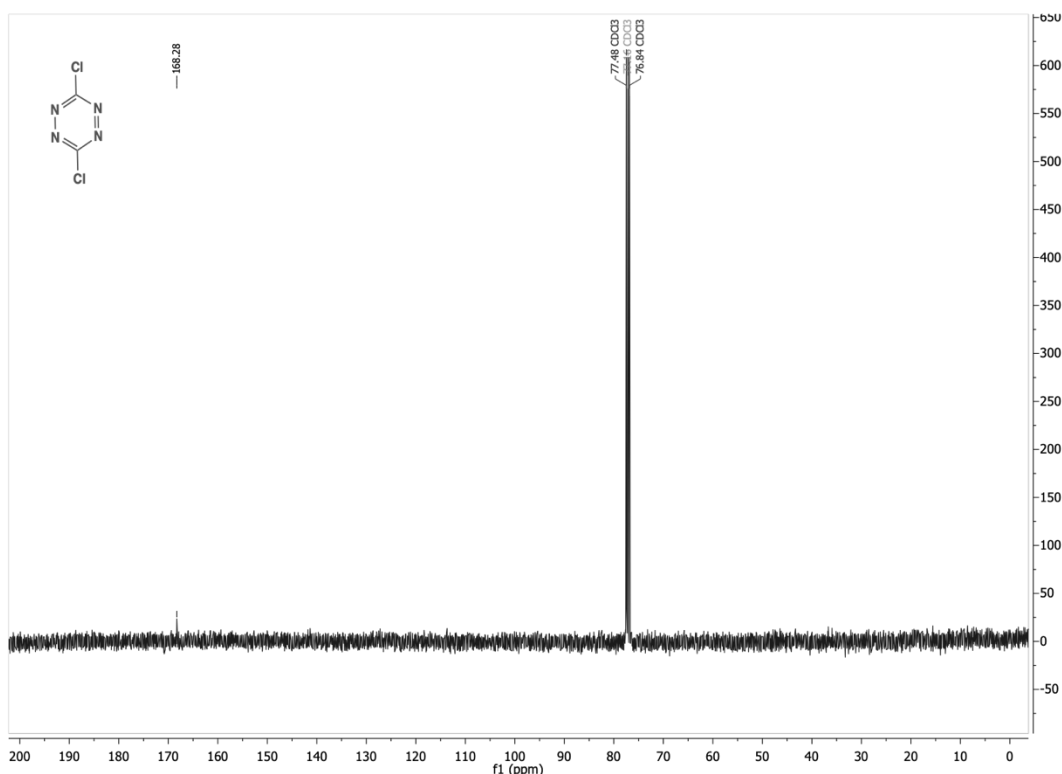

2. Synthesis of precursors

3,6-dichloro-1,2,4,5-tetrazine (1)
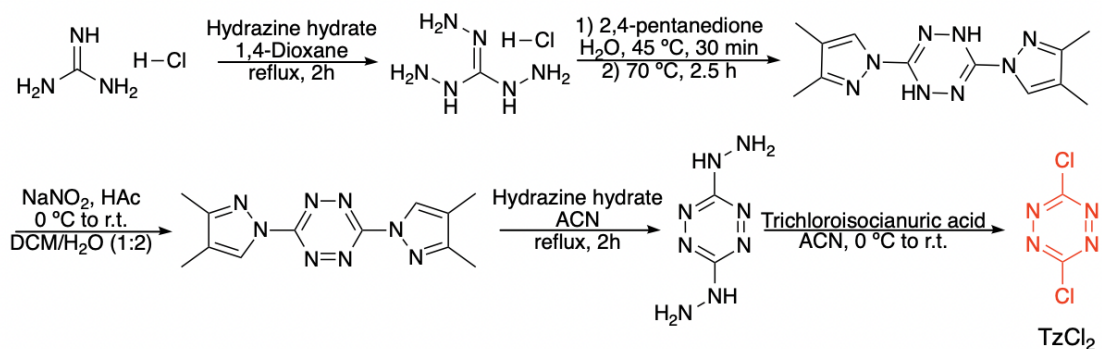
TzCl$_2$ was synthetized according to a previous published procedure by our group.[1]

^{13}C NMR (100 MHz, CDCl$_3$) δ 168.28.

4,4',4''-methanetriyltriphenol (2) [2]

(1)
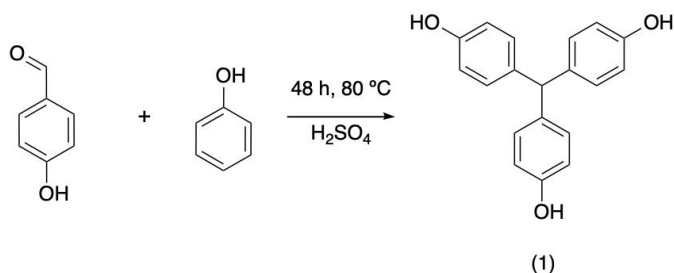
4-hydroxybenzaldehyde (2.4 g, 19.6 mmol) and phenol (11.1 g, 117,9 mmol) were placed in a 100 mL round bottom flask and heated at 50 °C until the phenol was completely melted. Then, a drop of H_2SO_4 was added and the mixture was heated at 80 °C for 48 h. After being cooled to room temperature, the crude was poured on brine (50 mL), extracted with EtOAc (3 x 50 mL), dried over Na_2SO_4, filtered, and concentrated on the rotavapor. The desired product was obtained as a light orange powder after being purified by column chromatography (Hex/Acetone 80:20). 4.14g, 72 %.

¹H NMR (500 MHz, Acetone-d_6) δ 8.15 (s, 3H), 6.91-6.93 (d, *J* = 8.6 Hz, 6H), 6.73-6.75 (d, *J* = 8.6 Hz, 6H), 5.32 (s, 1H).

¹³C NMR (126 MHz, Acetone-d_6) δ 155.58, 136.05, 130.07, 114.84, 54.33.

HRMS (ESI+, m/z): calculated for $C_{19}H_{15}O_3$ 291.1021; found 291.1021.
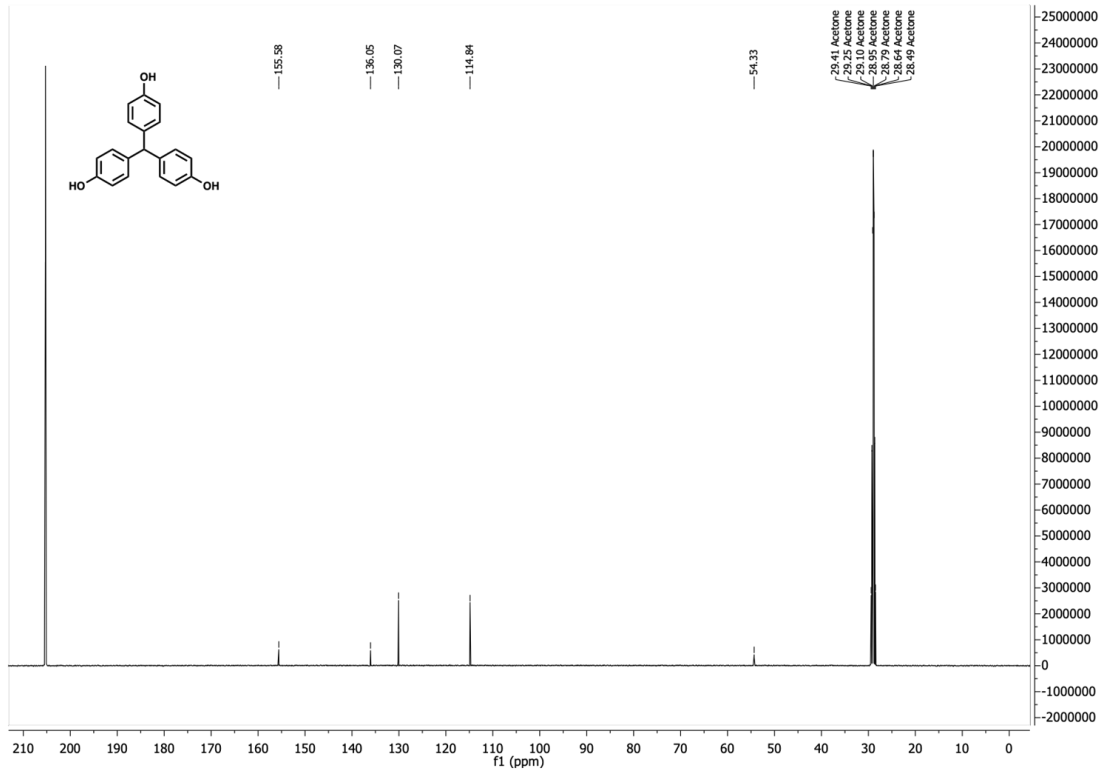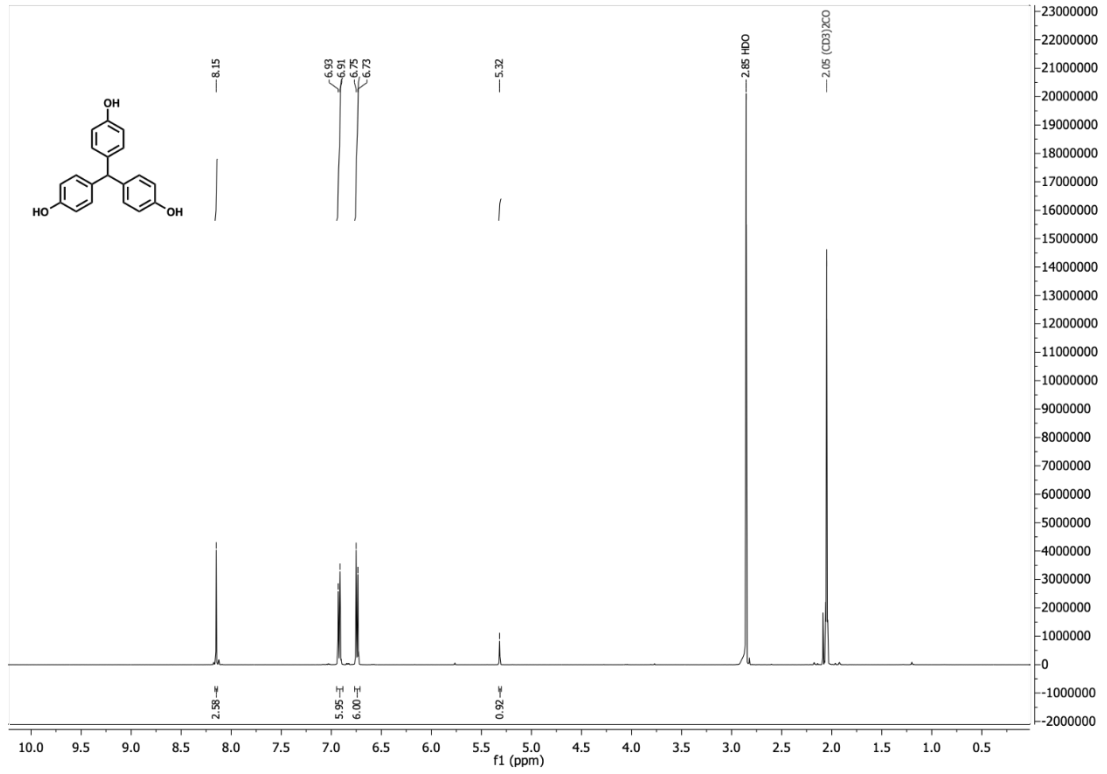
3. Polymer optimization

Several parameters were tested to evaluate the formation of polymer **P1**, taken as the standard reaction.

Solvents

All the reactions were developed in the following conditions (0.01M, TEA 4.5 eq).

SOLVENT	MORPHOLOGY	D (nm)	YIELD (%)
TOLUENE	shapeless + sphere	619±86	65
Et$_2$O	amorphous	-	14
THF	sphere	163±73	33
DCM	-	-	-
ACETONE	sphere	2898±260	20
ACN	sphere	1053±40	96
DMF	shapeless	-	75

Bases and concentration

Inorganic and organic bases were tested as well as different concentrations.

BASE	MORPHOLOGY	[M]	D (nm)	YIELD (%)
TEA	sphere	0.01	1053±40	96
DIPEA	sphere	0.01	921±58	90
DBU	sphere	0.01	94±24	71
DABCO	sphere	0.01	328±104	56
NMM	sphere	0.01	2247±646	33
Py	shapeless	0.01	-	86
2-NO$_2$-Py	-	0.01	-	-
DMAP	-	0.01	-	-
NaH	-	0.01	-	-
Cs$_2$CO$_3$	shapeless	0.01	-	5
TEA	sphere	0.1	1464±346	quant
TEA*	sphere	0.01	944±189	90
TEA	sphere	0.005	993±43	73
TEA	sphere	0.001	1323± 260	22

*Dropwise addition in 5 mL of ACN.

Molar ratio

Eq ROH	Eq TzCl$_2$	MORPHOLOGY	D (nm)	YIELD (%)
1	1.5	sphere	1053±40	96
1.5	1	-	-	-
1	1	heterogeneous sphere	678±34	25
0.5	1	heterogeneous sphere	1237±88	94
1	0.5	-	-	-
1	3	heterogeneous sphere	2201±981	32
3	1	-	-	-

7

Temperature

| T (°C)	TIME (h)	MORPHOLOGY	D (nm)	YIELD (%)
0	1	sphere	612±73	77
0	O.N.	sphere	600±90	47
25	O.N.	sphere	1035±40	96
50	1	sphere	880±56	63
70	O.N.	sphere	416±44	46

# 4. Synthesis and characterization of polymers

P1
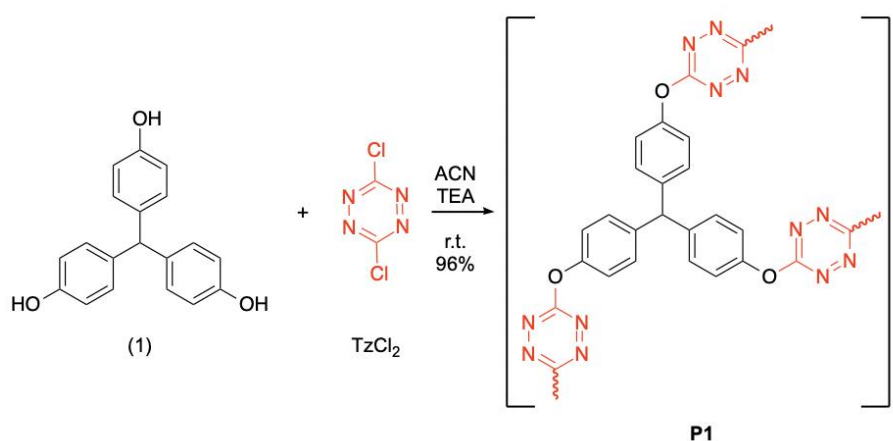
Phenol **(1)** (100 mg, 1 eq) and TzCl$_2$ (77.5 mg, 1.5 eq) were placed in a round bottom flask and dissolved in 35 mL of ACN (0.01 M). TEA (0.22 mL, 4.5 eq) was added and the solution changes from orange to red color. During the following 5 min the polymer started to precipitate and in 10 min the reaction was filtered. The pink solid was washed with ACN (2 x 20 mL), Milli-Q H$_2$O (2 x 20 mL), MeOH (2 x 20 mL) and vacuum dried for 5 min. Finally, the polymer was dried on a high vacuum pump for 3-4 h. 133.6 mg, 96 % yield. Anal. Calc. for (C$_{22}$H$_{13}$N$_3$O$_3$)·(H$_2$O)$_{0.25}$: C, 63.84; H, 3.29; N, 20.31; O, 12.56. Found: C, 63.79; H, 3.14; N, 20.57; O, 12.50.

IR analysis:

The characteristic band for the O-H stretching around 3250 cm^{-1} nearly disappears from black to blue spectra. Furthermore, near 1350 cm^{-1} there is a sharp signal characteristic of C-O stretching for ether compounds (blue) where previously was the O-H bending signal for phenols in the black spectra. Finally, it can be observed that the signals of TzCl$_2$ around 800 cm^{-1} for the C-Cl bond have also disappeared.
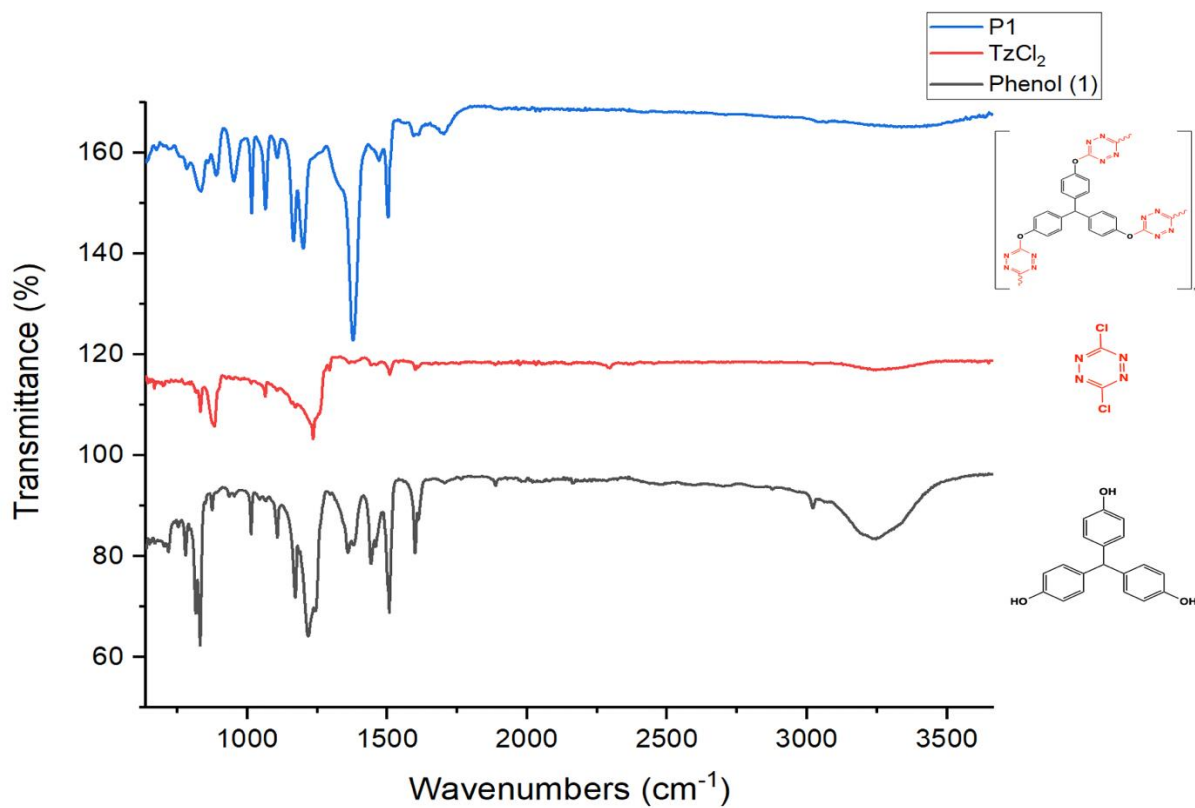
SEM Images:
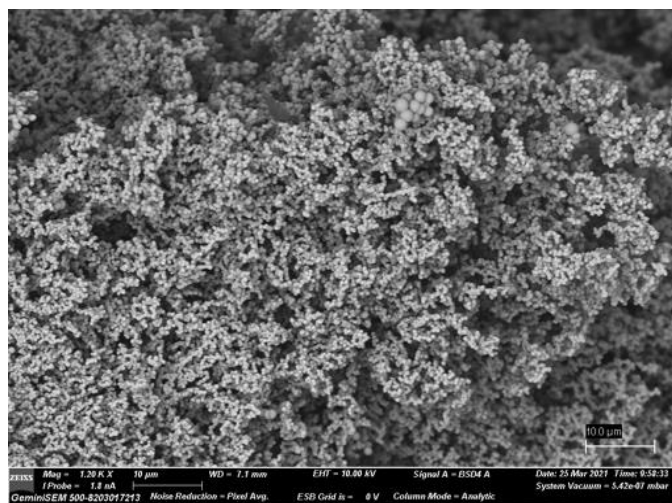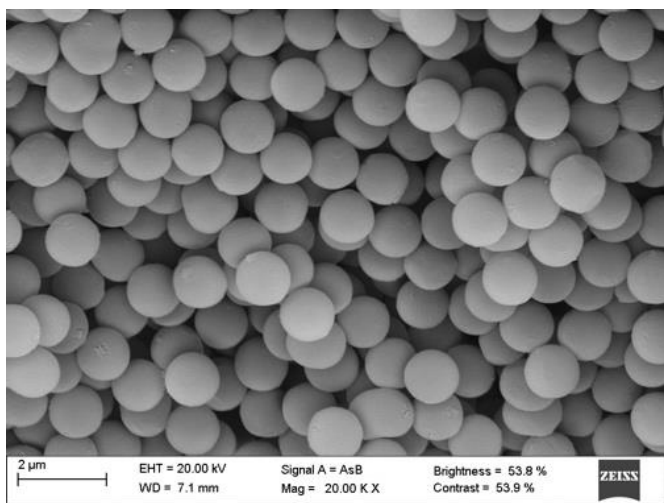
Solid-state ^{13}C-NMR:
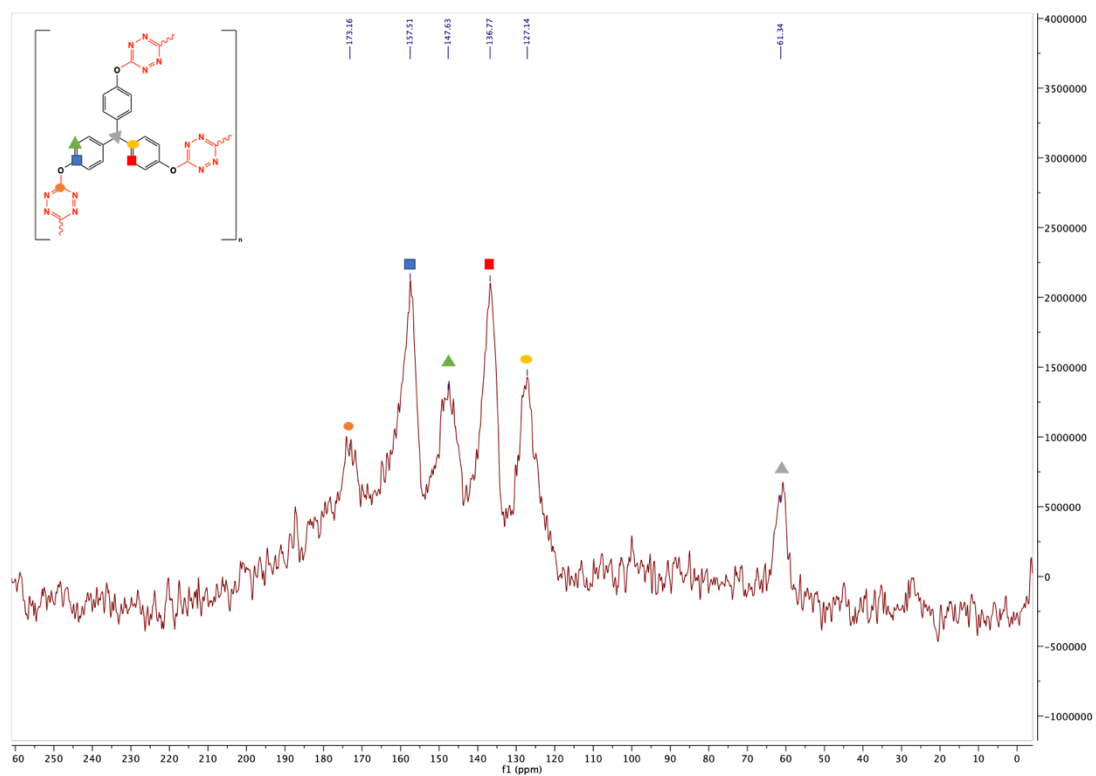
Solid state ^{13}C-NMR of P1
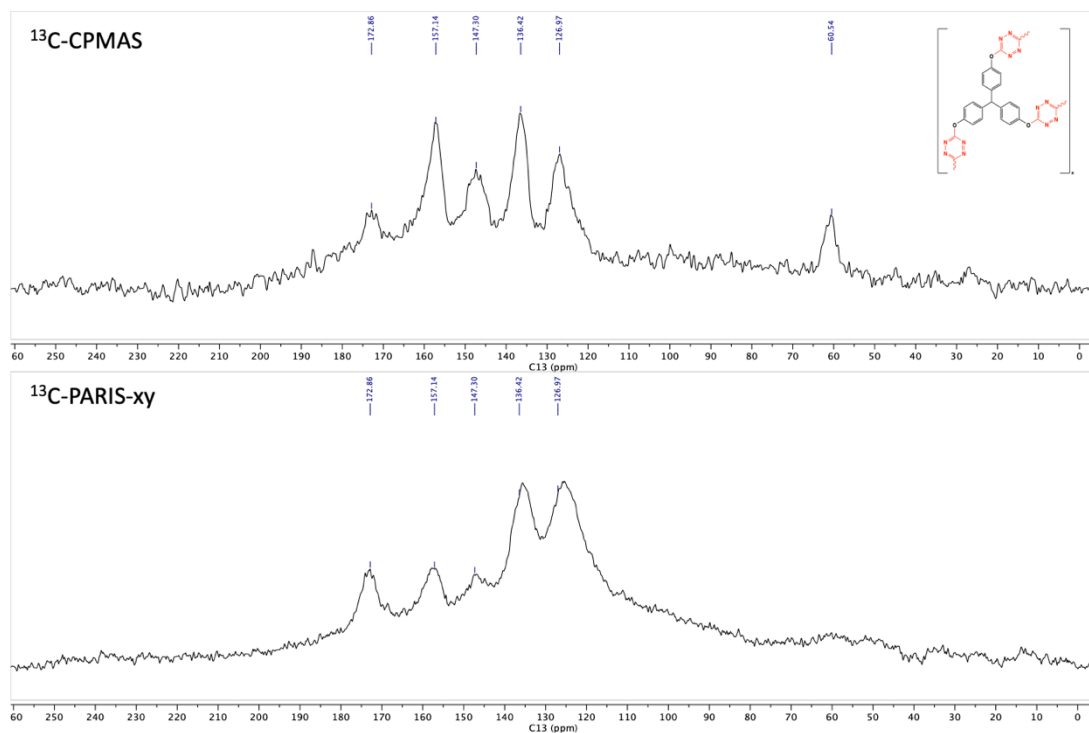
Solid state ^{13}C-NMR of P1. CPMAS vs PARIS-xy spectra.

BET analysis:

Surface Area (m²/g)	Pore Diameter (nm)
7.391	177.7

According to the pore diameter the material P1 can be designed as a macroporous solid.
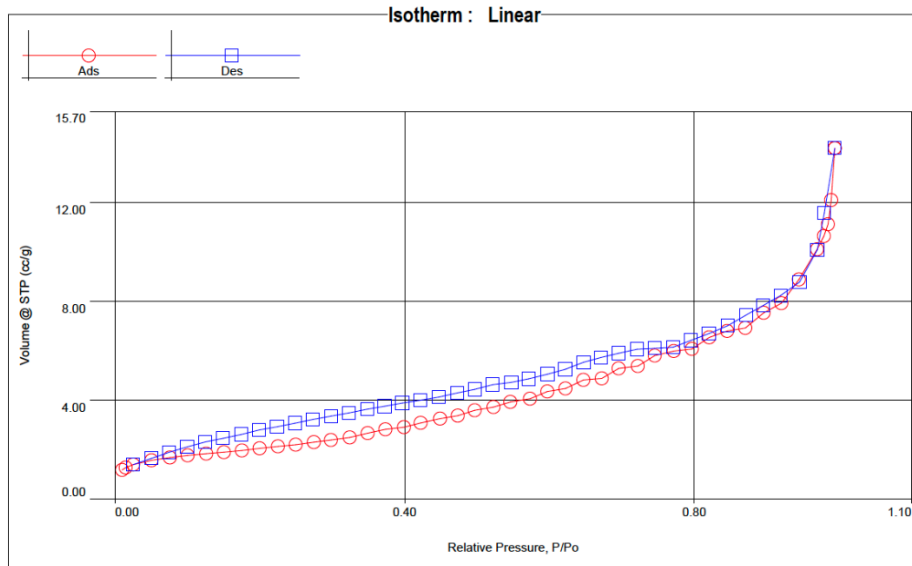
Linear isotherm of P1. Type III isotherm.
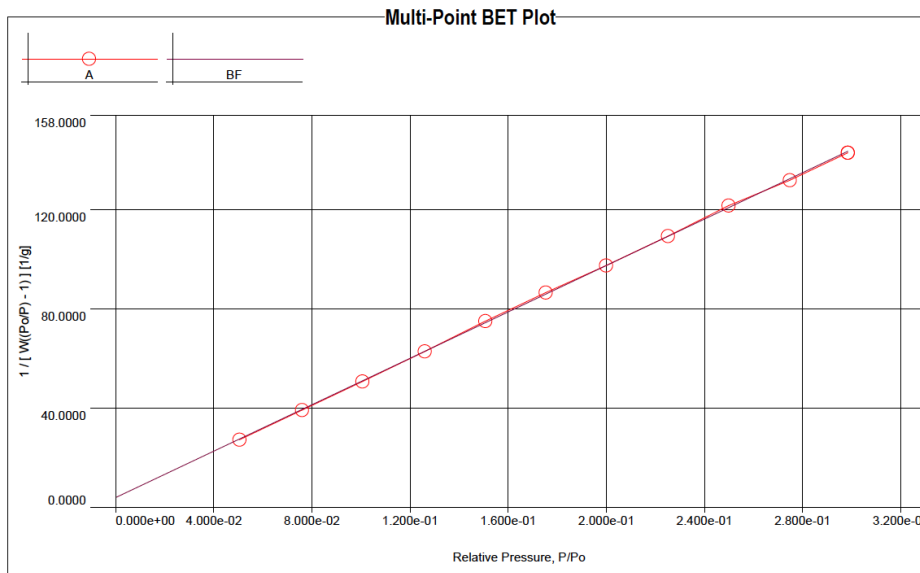
Multipoint BET plot of P1.

TGA analysis:

TGA/DTGA analysis for **P1** shows 2 main events. The first weight loss is about 19 %, meanwhile the second event implies an 81 % mass loss. DTGA is in concordance with these results: two exothermic processes around 324 and 612 °C. **T$_{5\%}$: 294 °C**
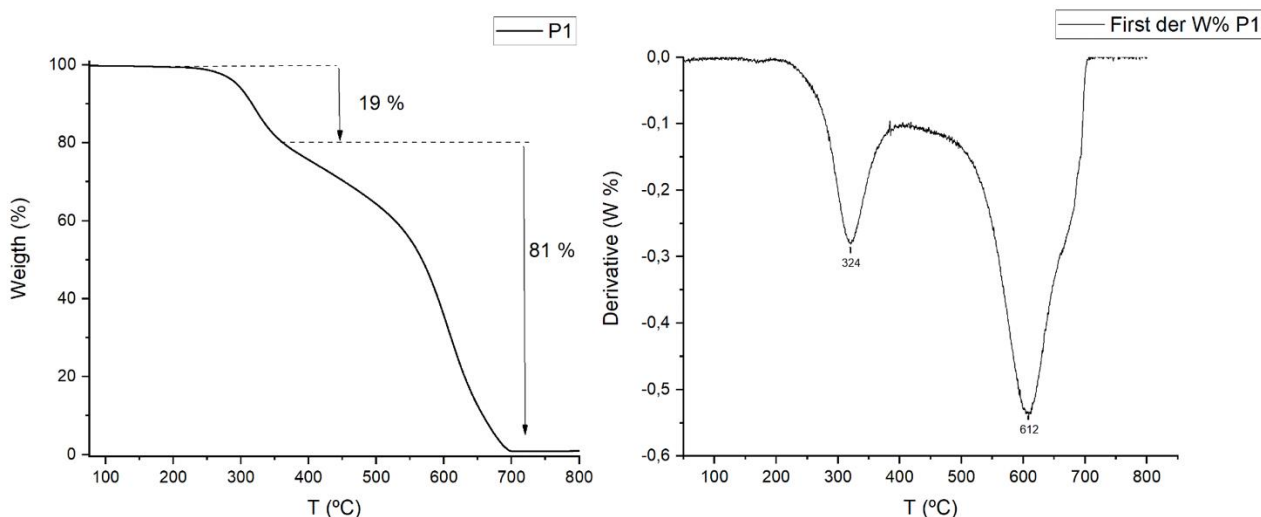
Cyclic Voltammetry (CV):

A three-electrode configuration was employed, with a Pt wire as the working electrode, glassy carbon as the counter electrode and Pt wire as the reference electrode. Tetrabutylammonium hexafluorophosphate (2 mM) was used as supporting electrolyte. The measurements were performed in ACN (0.5 mM) under Ar protection at ambient temperature. All samples were deoxygenated with Ar prior to measurement. The scan rate was 100 mV/s in cyclic voltammetry (CV) measurements.

According to the CV, the material **P1** undergo a reversible one-electron redox process which potentials are -0.58 V and -0.71 V.
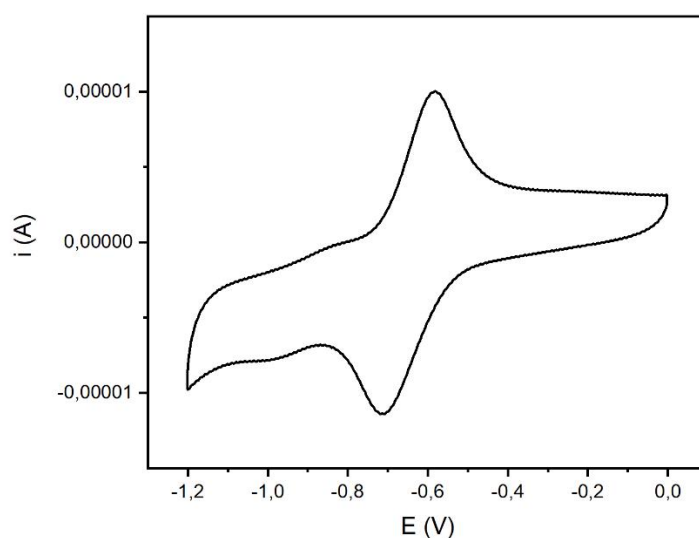
P2
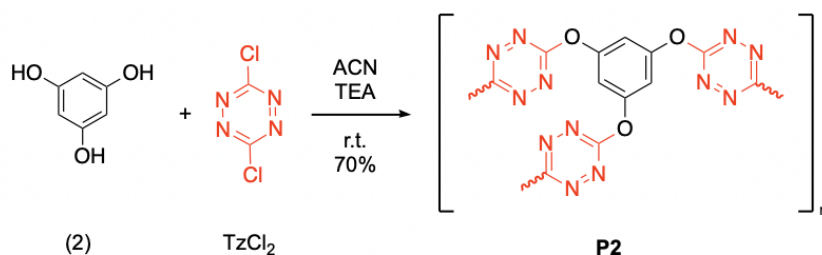

Phenol **(2)** (125 mg, 1 eq) and TzCl$_2$ (228 mg, 1.5 eq) were placed in a round bottom flask and dissolved in 100 mL of ACN (0.01 M). TEA (0.70 mL, 4.5 eq) was added. During the following 5 min the polymer started to precipitate and in 10 min the reaction was filtered. The pink solid was washed with ACN (2 x 20 mL), Milli-Q H$_2$O (2 x 20 mL), MeOH (2 x 20 mL) and vacuum dried for 5 min. Finally, the polymer was dried on a high vacuum pump for 3-4 h. 173.3 mg, 70 % yield. Anal. Calc. for (C$_9$H$_3$N$_6$O$_3$)·(H$_2$O)$_{0.7}$·(MeOH) $_{0.75}$: Calc. C, 41.85; H, 2.67; N, 30.04; O, 25.44. Found: C, 42.23; H, 2.58; N, 30.09; O, 25.10.

IR analysis:

The characteristic band for the O-H stretching around 3250 cm^{-1} nearly disappears from black to blue spectra. Furthermore, near 1300 cm^{-1} there is a broad signal characteristic of C-O stretching for ether compounds (blue) where previously was the O-H bending signal for phenols in the black spectra. Finally, it can be observed that the signals of TzCl$_2$ around 800 cm^{-1} for the C-Cl bond have also disappeared.
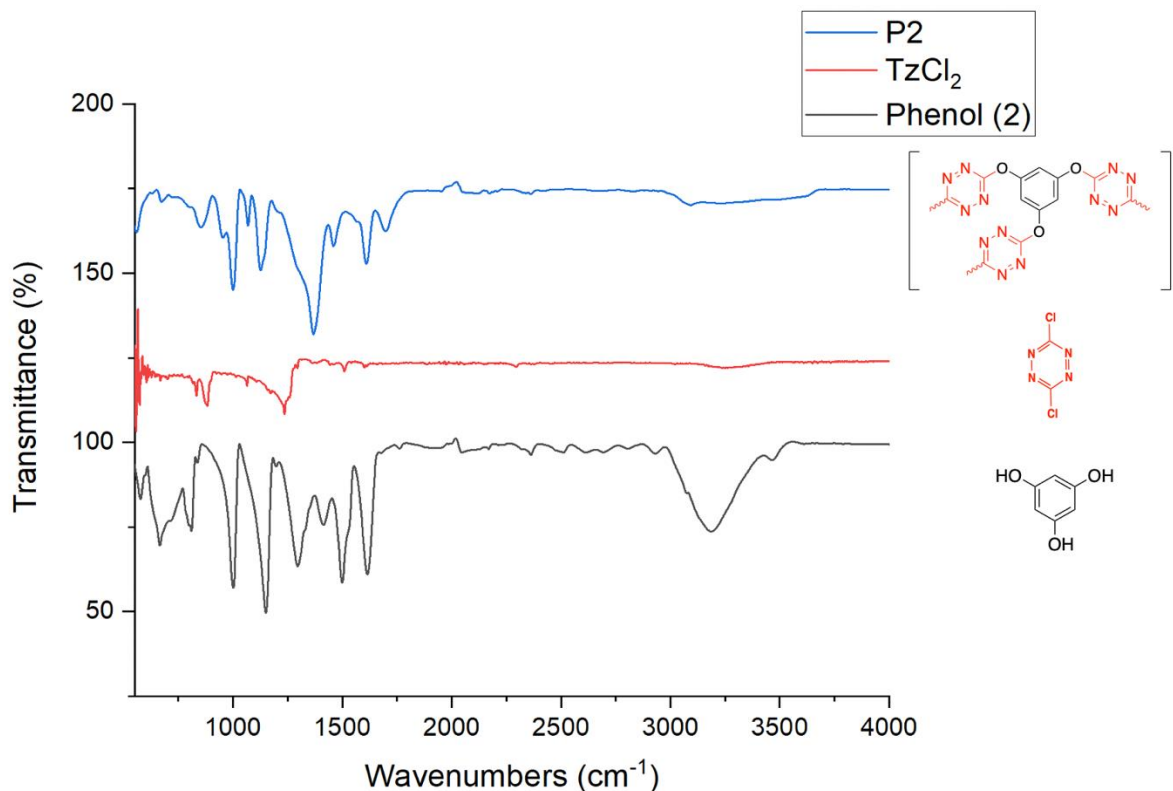
SEM images:
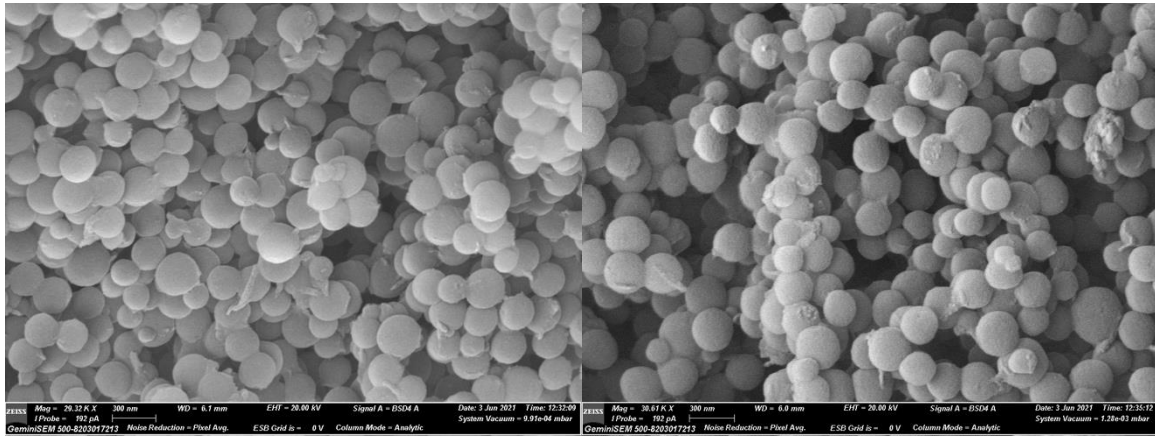
## TGA analysis:

TGA/DTGA analysis for **P2** shows 5 events. The first weight loss is about 4 % probably due to a loss of humidity. The second event implies an 9 % mass loss. Third event is about 27 %, fourth 46 % and the final one 14 %. DTGA is in concordance with these results: five exothermic processes around 235, 302, 405 and 675 °C. **$T_{5\%}$: 192 °C**

P3
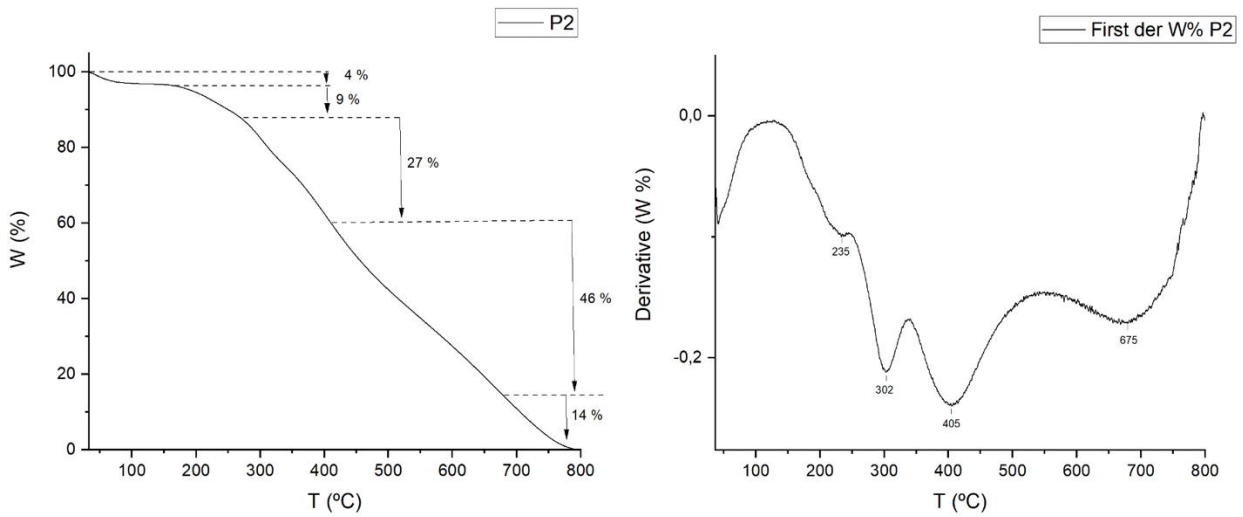
P3
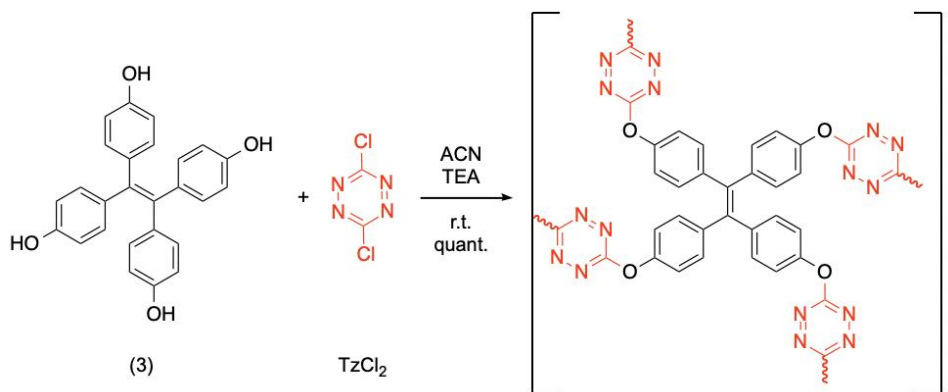
Phenol **(3)** (104 mg, 1 eq) and TzCl$_2$ (79 mg, 2 eq) were placed in a round bottom flask and dissolved in 26 mL of ACN (0.01 M). TEA (0.22 mL, 4.5 eq) was added. During the following 5 min the polymer started to precipitate and in 10 min the reaction was filtered. The pink solid was washed with ACN (2 x 20 mL), Milli-Q H$_2$O (2 x 20 mL), MeOH (2 x 20 mL) and vacuum dried for 5 min. Finally, the polymer was dried on a high vacuum pump for 3-4 h. 143 mg, quant. Anal. Calc. for (C$_{30}$H$_{16}$N$_8$O$_4$): C, 65.22; H, 2.92; N, 20.28; O, 11.58. Found: C, 65.26; H, 3.31; N, 20.01; O, 11.42.

IR analysis:

The characteristic band for the O-H stretching around 3250 cm^{-1} nearly disappears from black to blue spectra. Around 1650 cm^{-1} (blue) can be observed a weak peak typical of tetrasubstituted alkenes that in the black spectra is much more intense. Furthermore, near 1300 cm^{-1} there is a broad signal characteristic of C-O stretching for ether compounds (blue) where previously was the O-H bending signal for phenols in the black spectra. Finally, it can be observed that the signals of TzCl$_2$ around 800 cm^{-1} for the C-Cl bond have also disappeared.
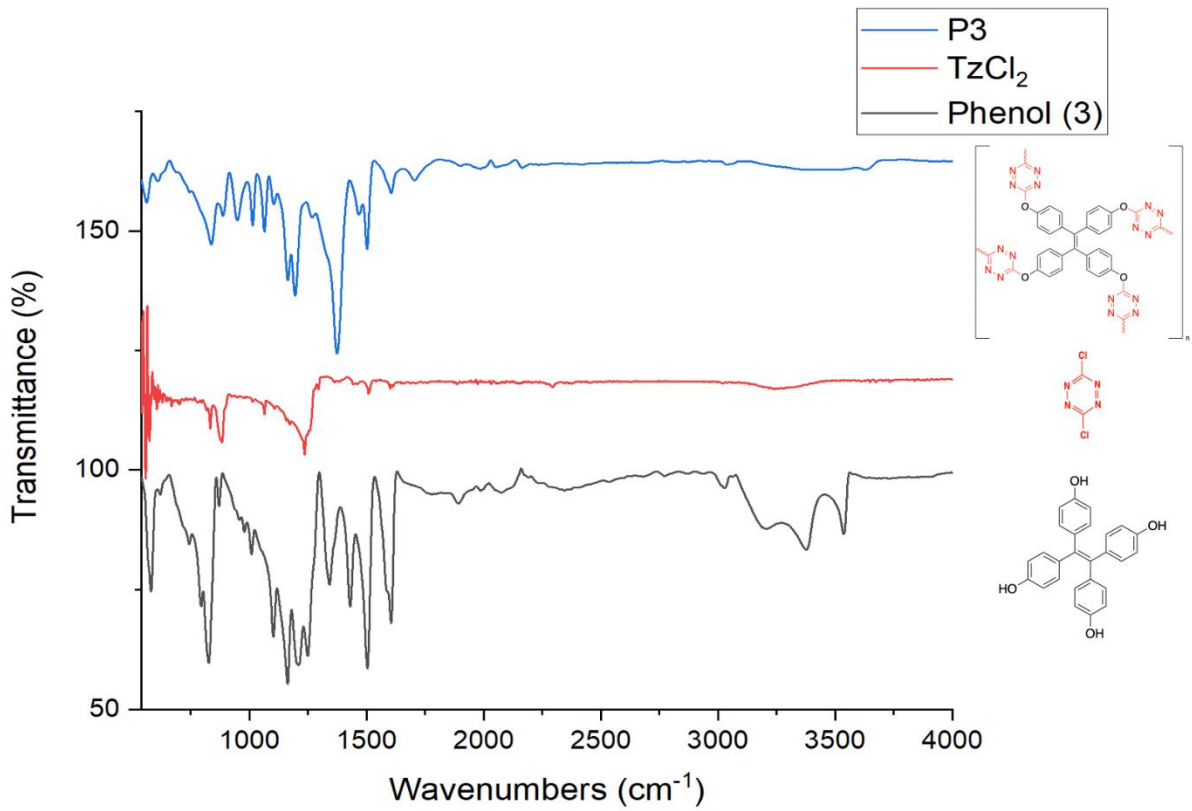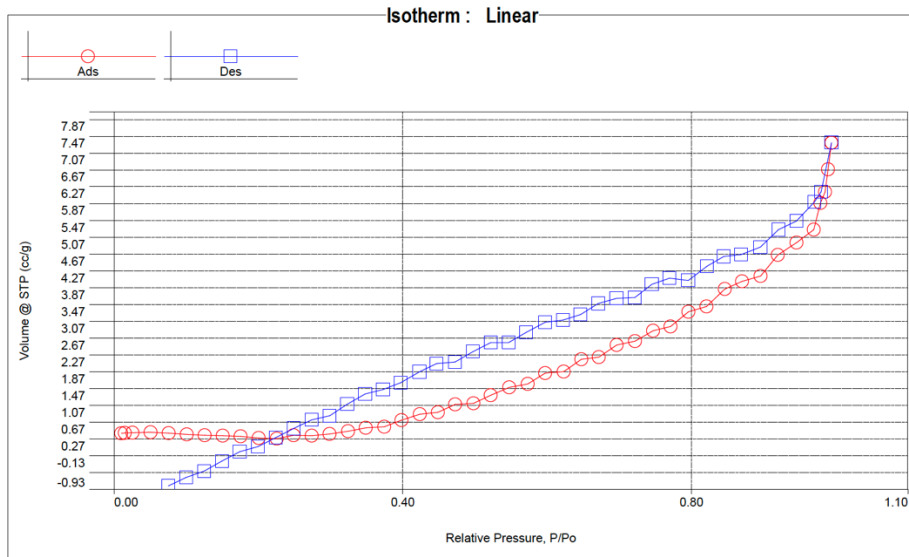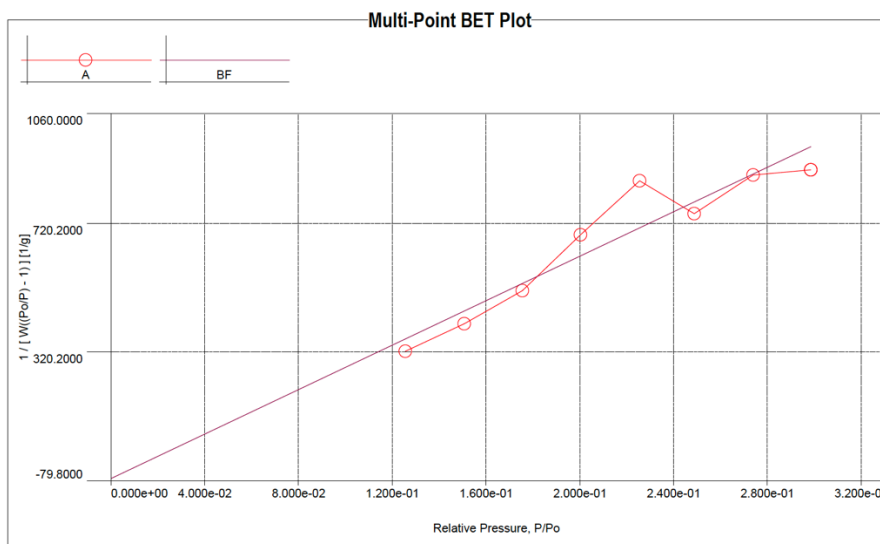
SEM images:
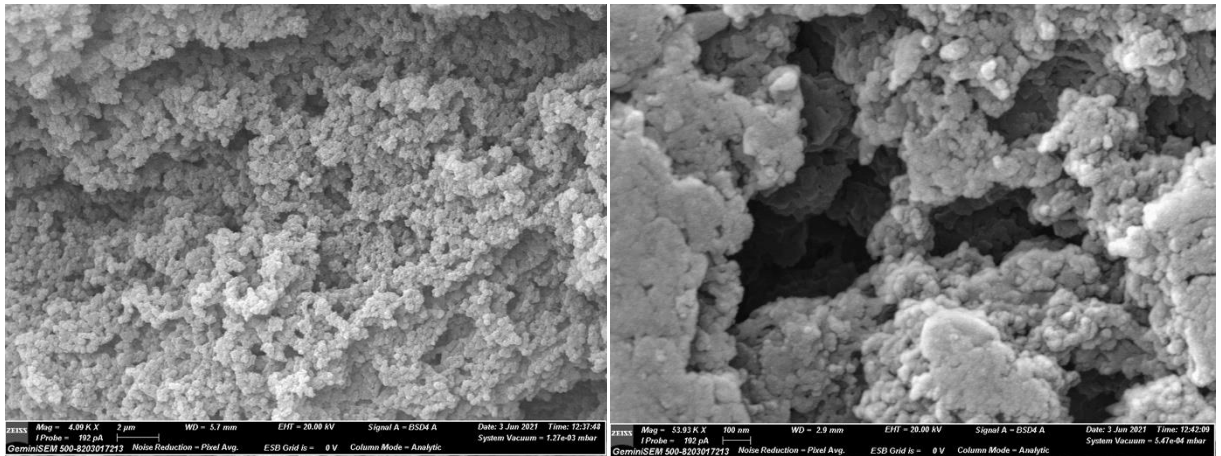
TGA analysis:

TGA/DTGA analysis for **P3** reveals 4 events. The first weight loss is about 4 % probably due to a loss of humidity. The second event implies an 8 % mass loss. Third event is about 12 % and the fourth one 26 %. From this point around 50 % mass loss continues to higher temperatures. DTGA is in concordance with these results: four exothermic processes around 188, 354, 455 and 663 °C. **$T_{5\%}$: 262 °C**

P4
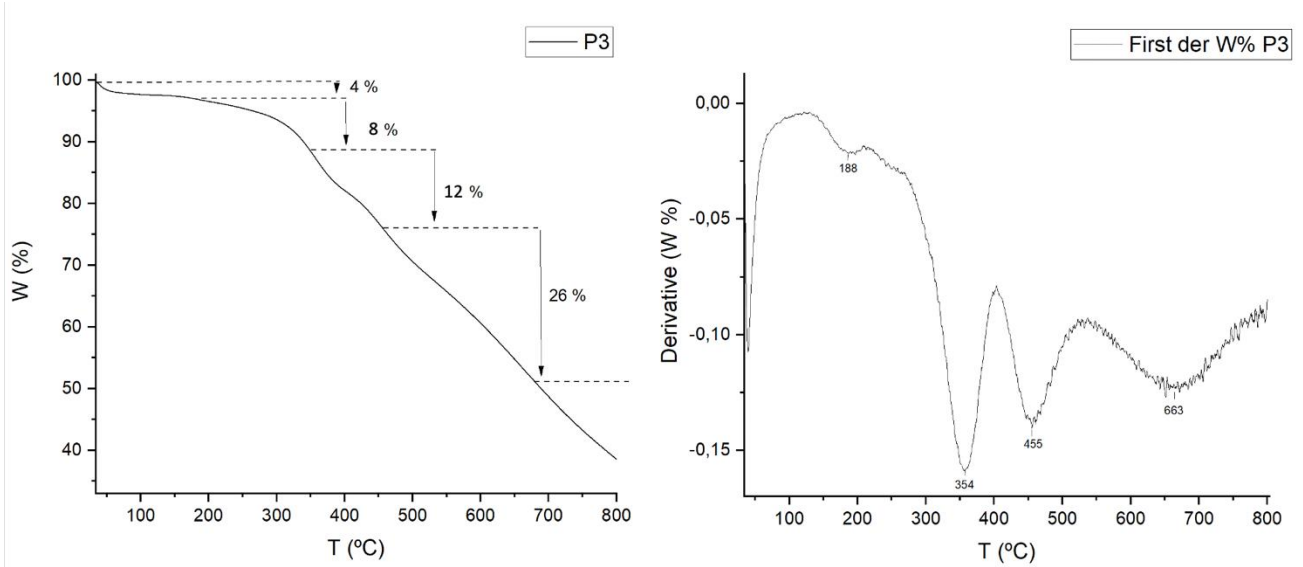
P4
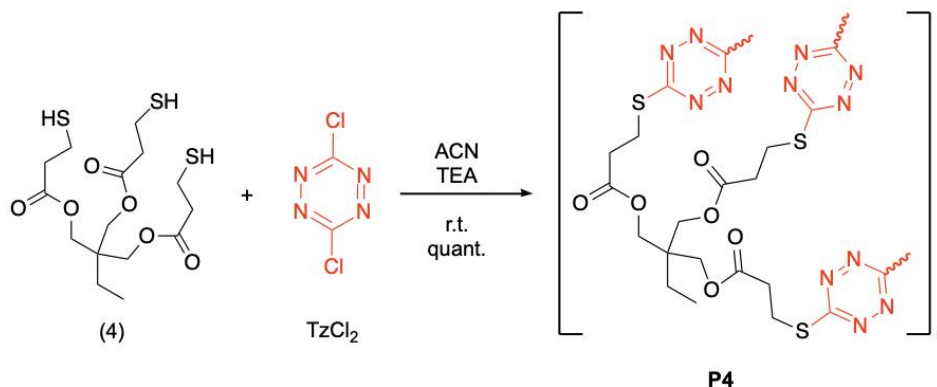
Commercially available thiol **(4)** (0.83 mL, 1 eq) and TzCl$_2$ (57.0 mg, 1.5 eq) were placed in a round bottom flask and dissolved in 25 mL of ACN (0.01 M). TEA (0.16 mL, 4.5 eq) was added and the solution changes from orange to red color. During the following 5 min. the polymer started to precipitate and in 10 min the reaction was filtered. The red solid was washed with ACN (2 x 20 mL), Milli-Q H$_2$O (2 x 20 mL), MeOH (2 x 20 mL) and vacuum dried for 5 min. Finally, the polymer was dried on a high vacuum pump for 3-4 h. 137.5 mg, quantitative yield. Anal. Calc. for (C$_{18}$H$_{23}$N$_6$O$_6$S$_3$)·(MeOH)$_{0.25}$·(ACN)$_{0.05}$: C, 41.92; H, 4.64; N, 16.10; O, 19.06; S, 18.27. Found: C, 42.31; H, 4.52; N, 15.71; O, 19.44; S, 18.02.

IR analysis:

The characteristic band for the S-H stretching around 2650 cm^{-1} nearly disappears from black to blue spectra. Around 2900-3000 cm^{-1} (blue) it can be observed a weak peak typical of alkane C-H stretching that in the black spectra is much more intense. Furthermore, a very strong band near 1750 cm^{-1} typical of C=O stretching can be observed in blue and black spectra and around 1250 cm^{-1} the sharp signal for C-O stretching of the ester moiety. Finally, it can be observed that the signals of TzCl$_2$ around 800 cm^{-1} for the C-Cl bond have also disappeared.
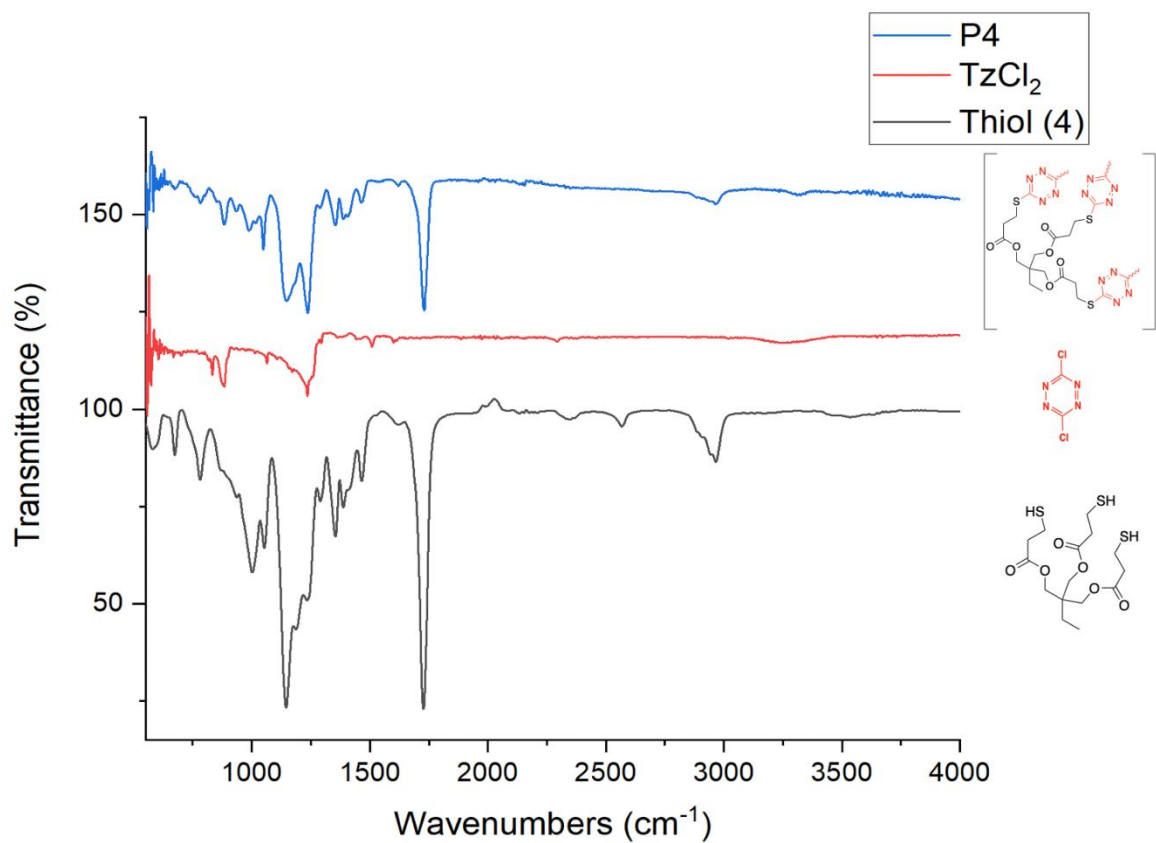
SEM images:
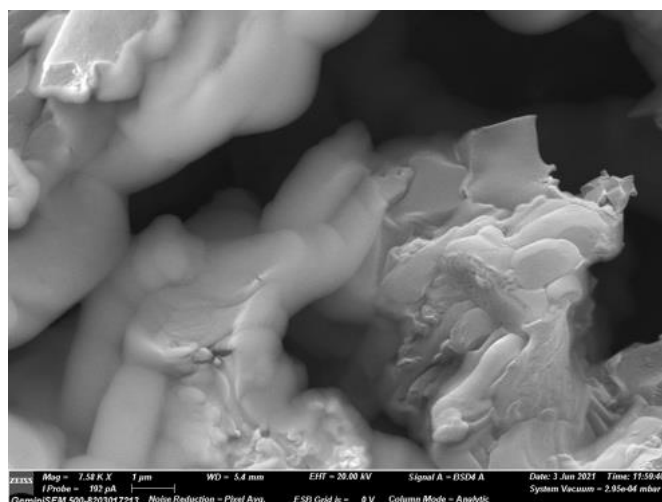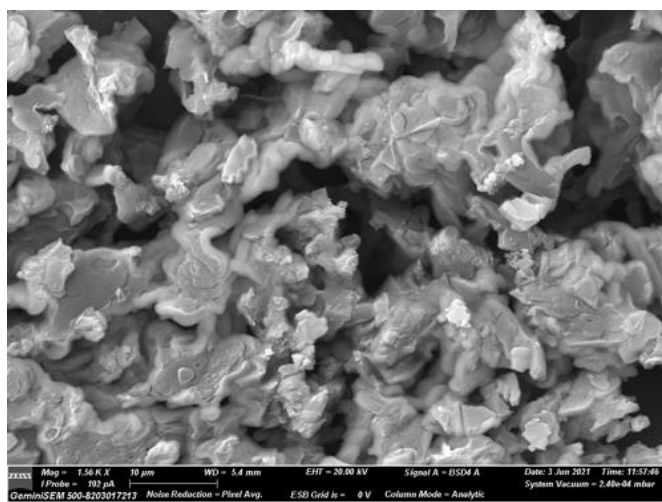
BET analysis:

Surface Area (m²/g)	Pore Diameter (nm)
1.031	183.8

According to the pore diameter the material P4 can be designed as a macroporous solid.

Linear isotherm of P4. Type IV isotherm.

Multipoint BET plot of P4.

TGA analysis:

TGA/DTGA analysis for **P4** shows 3 main events. The first weight loss is about 1 %, probably due to a loss of humidity. The second is about 20 % meanwhile the third one implies a 60 % mass loss. The last event is about 19 % weight loss. DTGA is in concordance with these results: 3 exothermic processes around 245, 361 and 606 °C. **T$_{5\%}$: 232 °C**

P1_DA
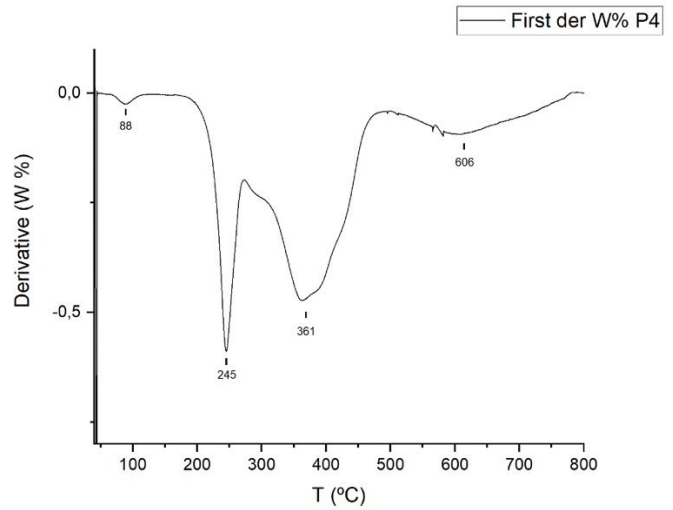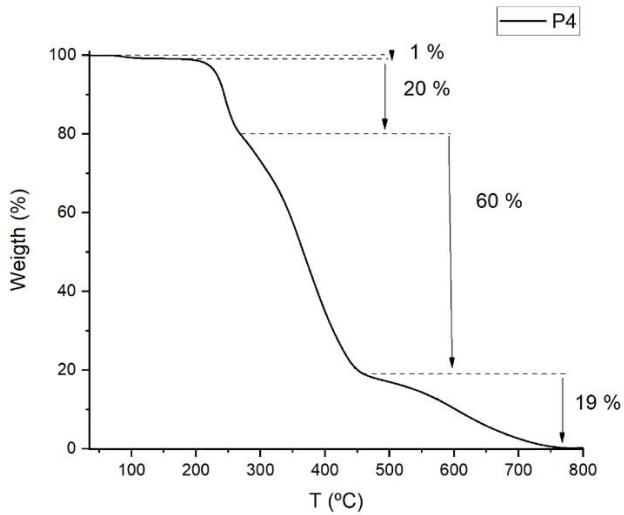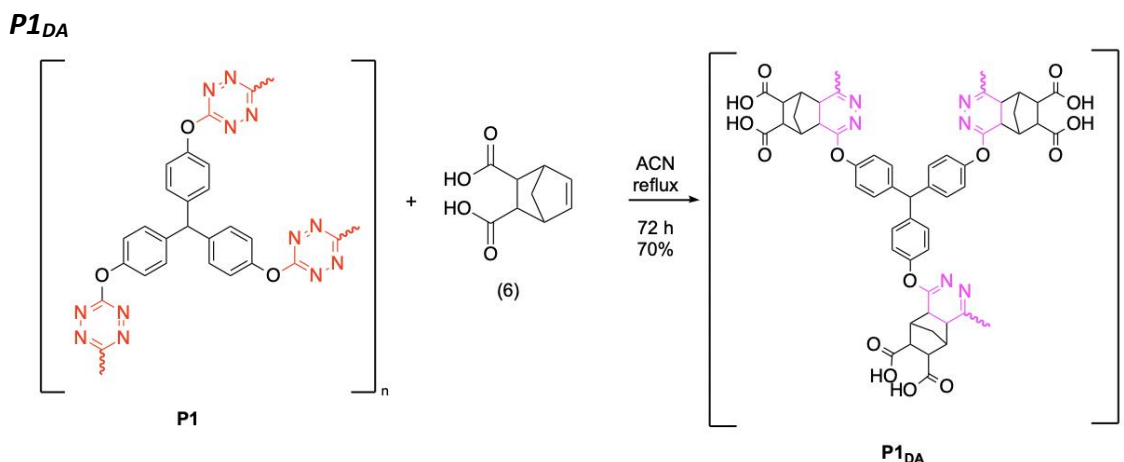
P1 (100 mg, 1 eq) and *cis*-5-norbornene-endo-2,3-dicarboxylic acid **(6)** (445 mg, 10 eq) were placed in a round bottom flask and refluxed for 72 h in 25 mL of ACN (0.01 M). The solution was cooled to room temperature and the obtained brown solid was filtered and washed with ACN (2 x 20 mL), Milli-Q H_2O (2 x 20 mL), MeOH (2 x 20 mL) and vacuum dried for 5 min. Finally, the polymer was dried on a high vacuum pump for 3-4 h. 109 mg of solid obtained, 70%. Calc. for ($C_{35.5}H_{25}N_3O_9$): C, 66.87; H, 3.95; N, 6.59; O, 18.62. Found: C, 52.27; H, 4.59; N, 7.00; O, 36.15. This divergence in the elemental analysis implies that some of the tetrazine rings do not react.

Water solubility modulation by post-functionalization
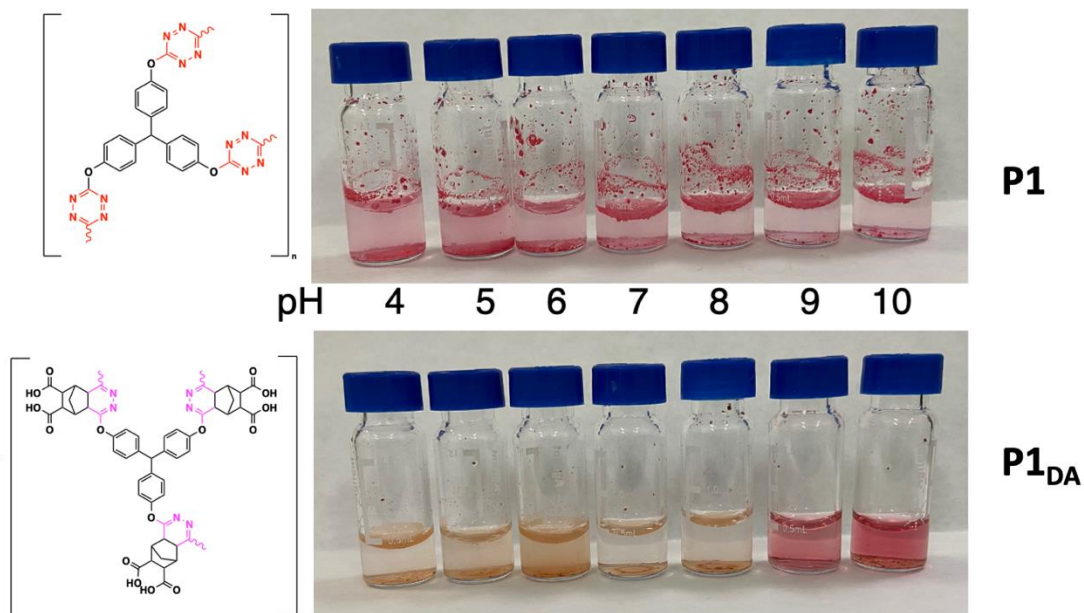
Image of P1 and P1_DA in a different pH range.

22

IR analysis:

IR comparative spectra of **P1** and the IEDDA obtained product **P1$_{DA}$**. The red spectra of P1$_{DA}$ show some characteristic signals like: O-H stretching band around 3100 cm^{-1} for carboxilic acid H; a medium-broad band near 1800 cm^{-1} typical of C=O stretching; also, near 1350 cm^{-1} there is a medium-sharp signal characteristic of C-O stretching for ether type compounds.
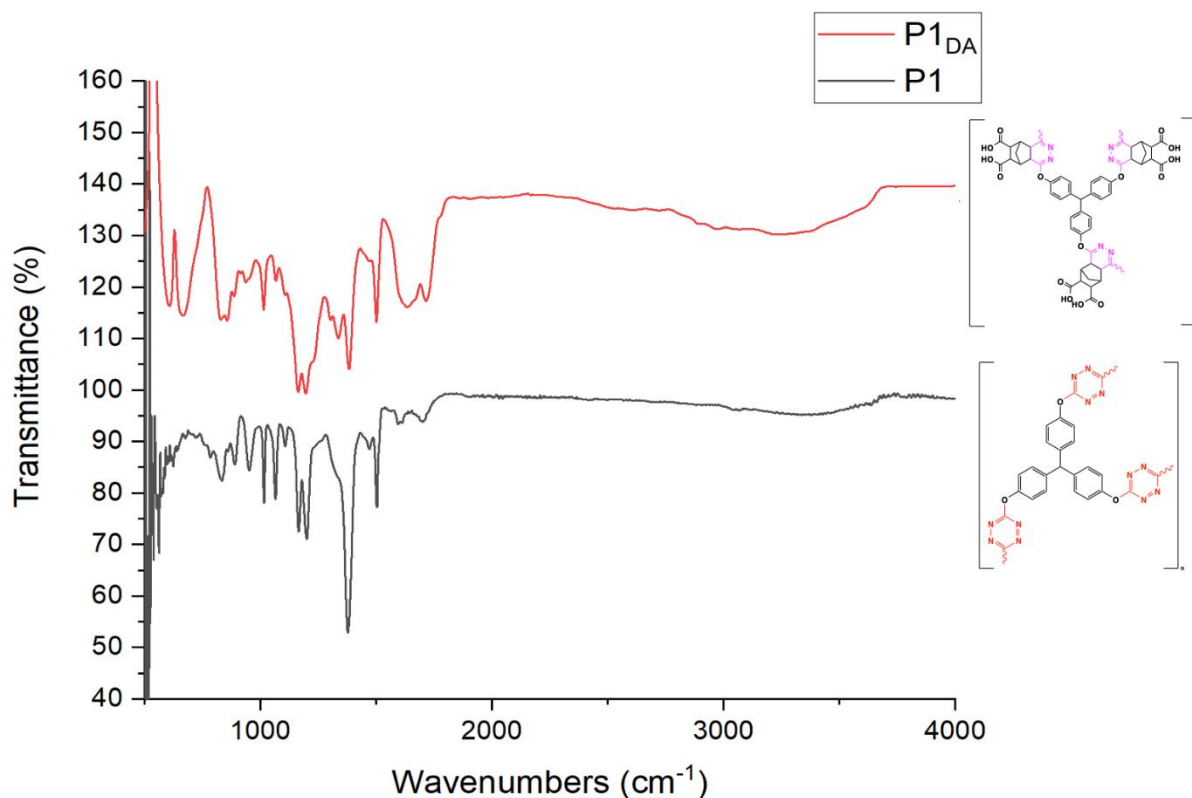
SEM images:
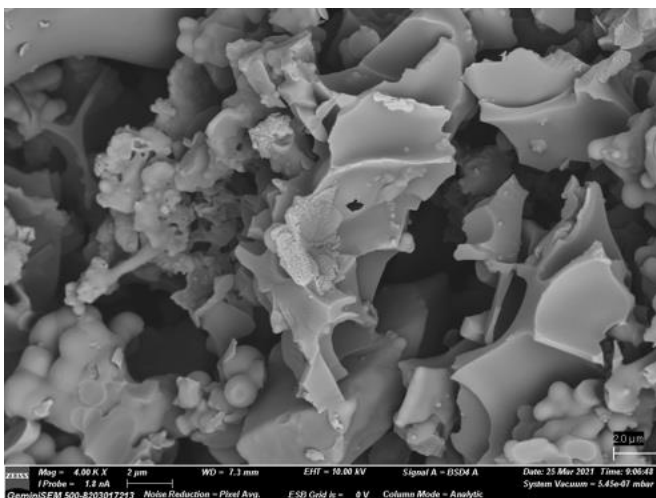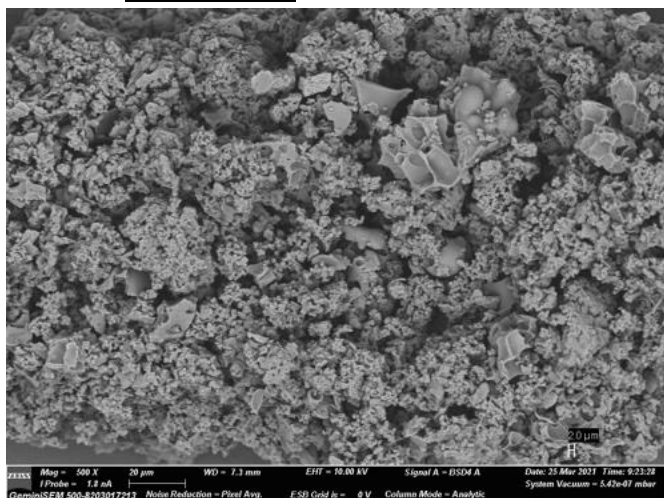
Solid-state ^{13}C-NMR:
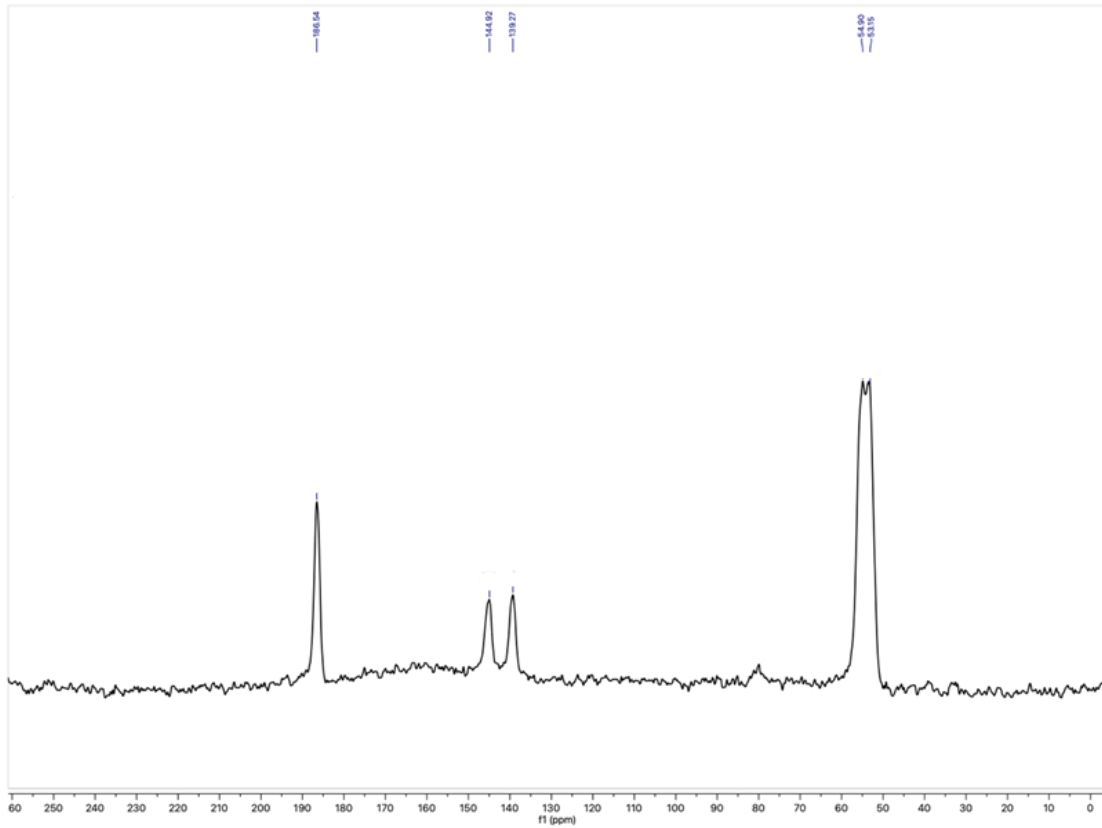
Solid state ^{13}C-NMR of P1$_{DA}$

BET analysis:

Surface Area (m²/g)	Pore Diameter (nm)
4.370	188.9

According to the pore diameter the material **P1$_{DA}$** can be designed as a macroporous solid.
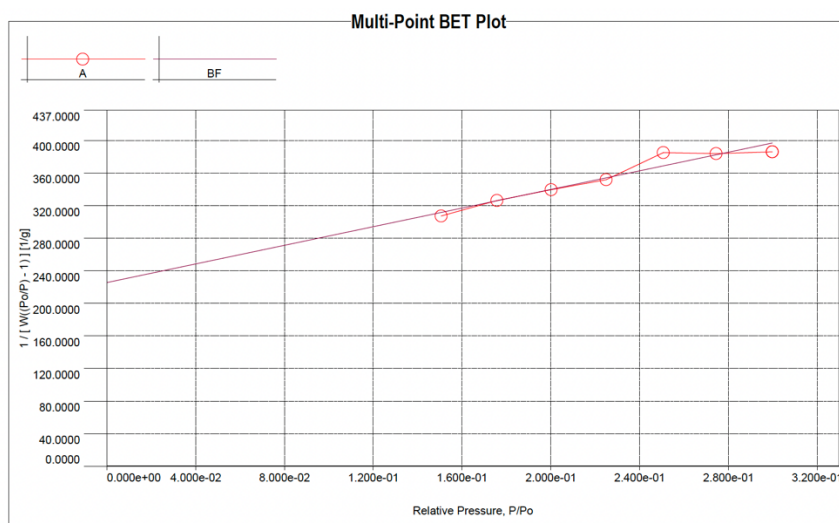
Multi-point BET plot of P1$_{DA}$.

TGA analysis:

TGA/DTGA analysis for **P1$_{DA}$** shows 3 main events and a first process due to loss of volatiles. The first weight loss is about 2 %. The second event implies a 10 % mass loss and finally a 34 %. From this point around 42 % the mass loss continues to higher temperatures. DTGA is in concordance with these results: 2 exothermic processes around 296 and 432 °C. **T$_{5\%}$: 145 °C**
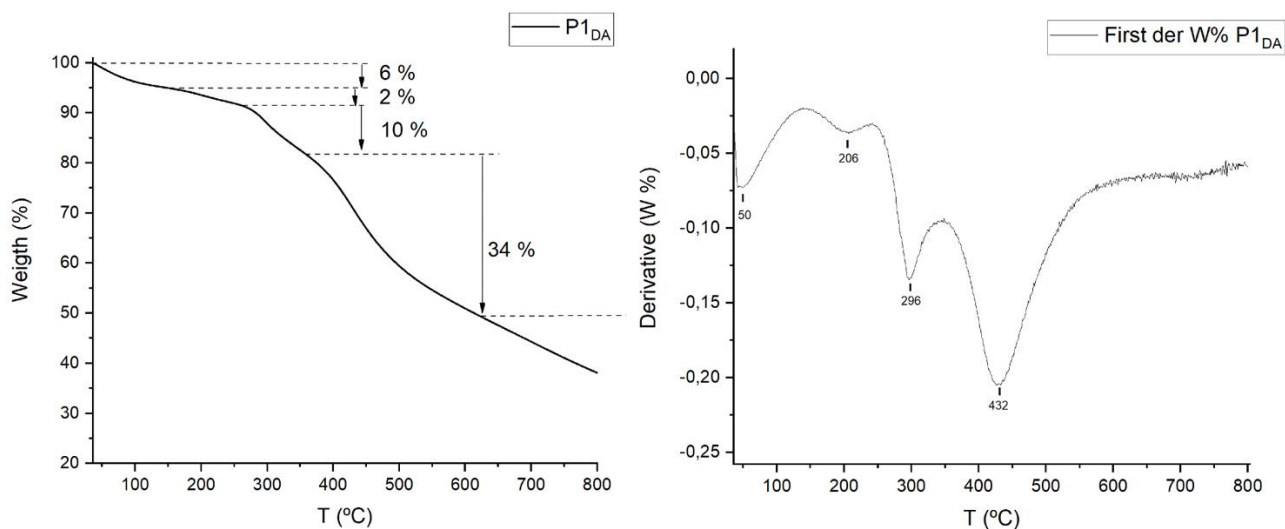
Post-Stabilization:

Diels-Alder reaction of **P1** with the norbornene acid derivate avoid degradation induced by dodecanethiol and triethylamine. Indeed, the polymer remained intact and the [1]H-

NMR of the solution only showed peaks from dodecanethiol and TEA, but no phenol **1** was detected, even after 24h.
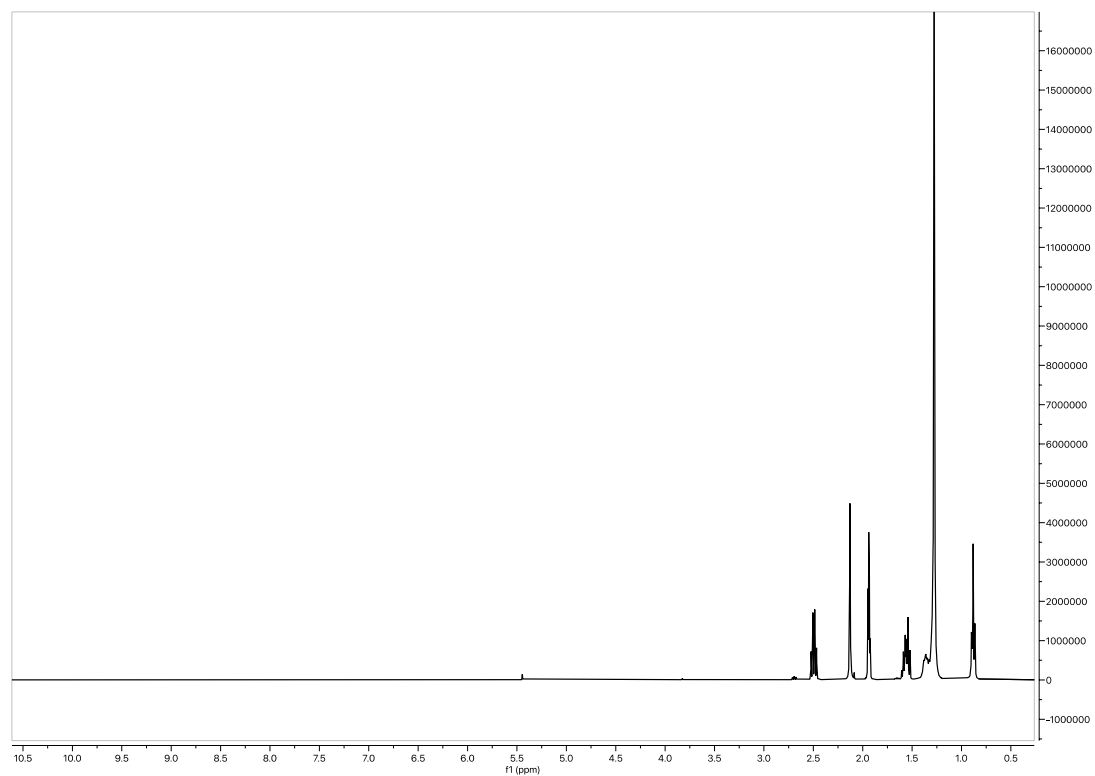
Degradation experiment with P1$_{DA}$ in presence of dodecanthiol. Only the latter is observed in solution.

P1_{RED}
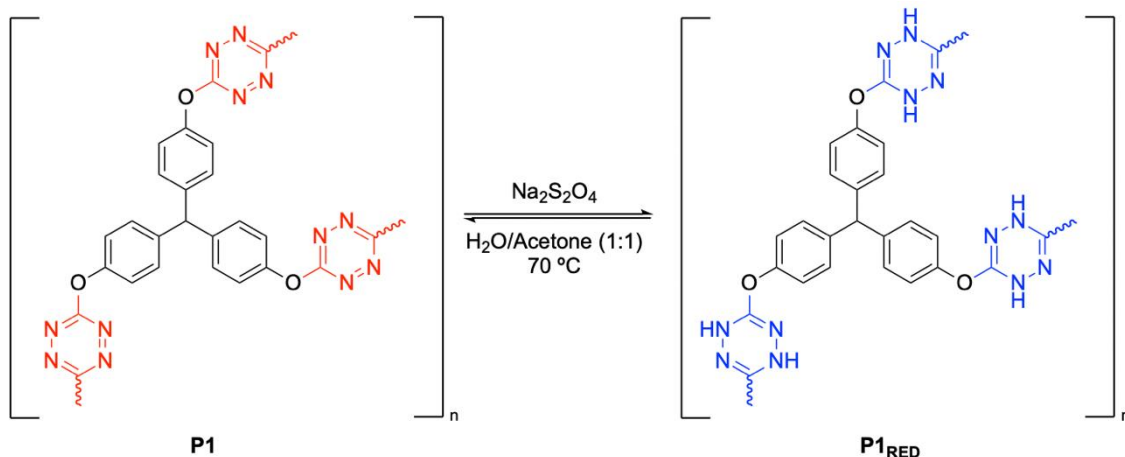
P1 (90 mg, 1 eq) and sodium dithionite (235 mg, 6 eq) were placed in a round bottom flask and refluxed for 24 h in a 1:1 acetone/water mixture (22 mL, 0.01 M). The solution was cooled to room temperature and the obtained white solid was filtered and washed with ACN (2 x 20 mL), Milli-Q H_2O (2 x 20 mL), MeOH (2 x 20 mL) and vacuum dried for 5 min. Finally, the polymer was dried on a high vacuum pump for 3-4 h. 55 mg, 60 % yield.

NOTE: This polymer rapidly reoxidizes by air contact. The reduction was confirmed by IR.

IR analysis:

The reduction reaction exposed a similar spectrum for **P1**_{RED} and **P1**, except the characteristic peaks for the N-H stretching of the reduced tetrazine around 3300 cm^{-1} and the new C-N stretching near 1250 cm^{-1}.
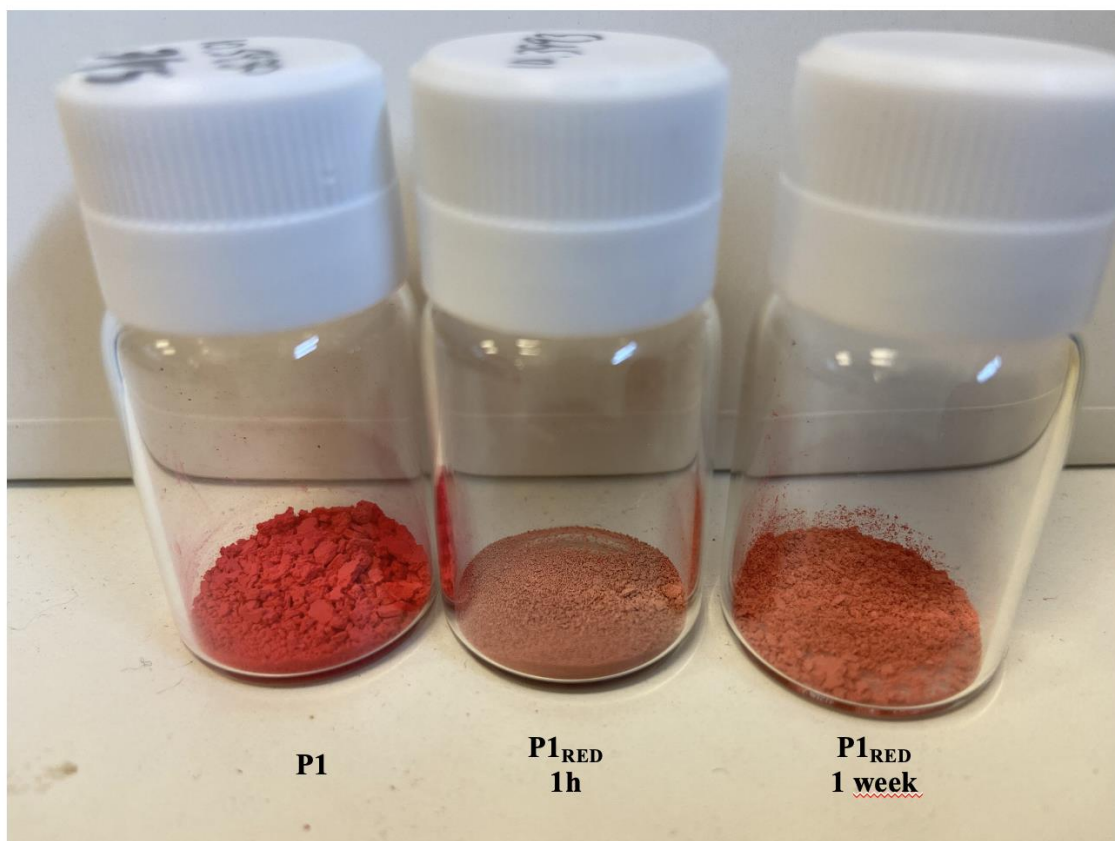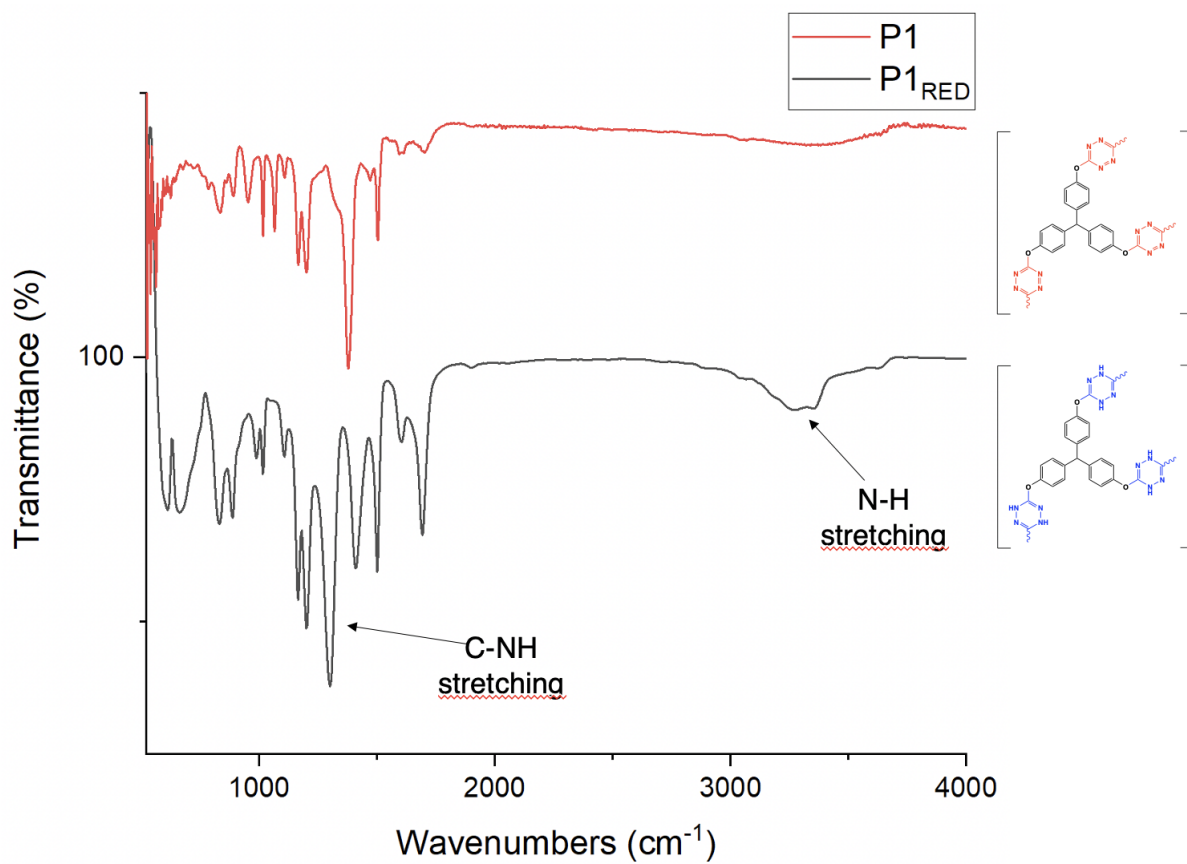
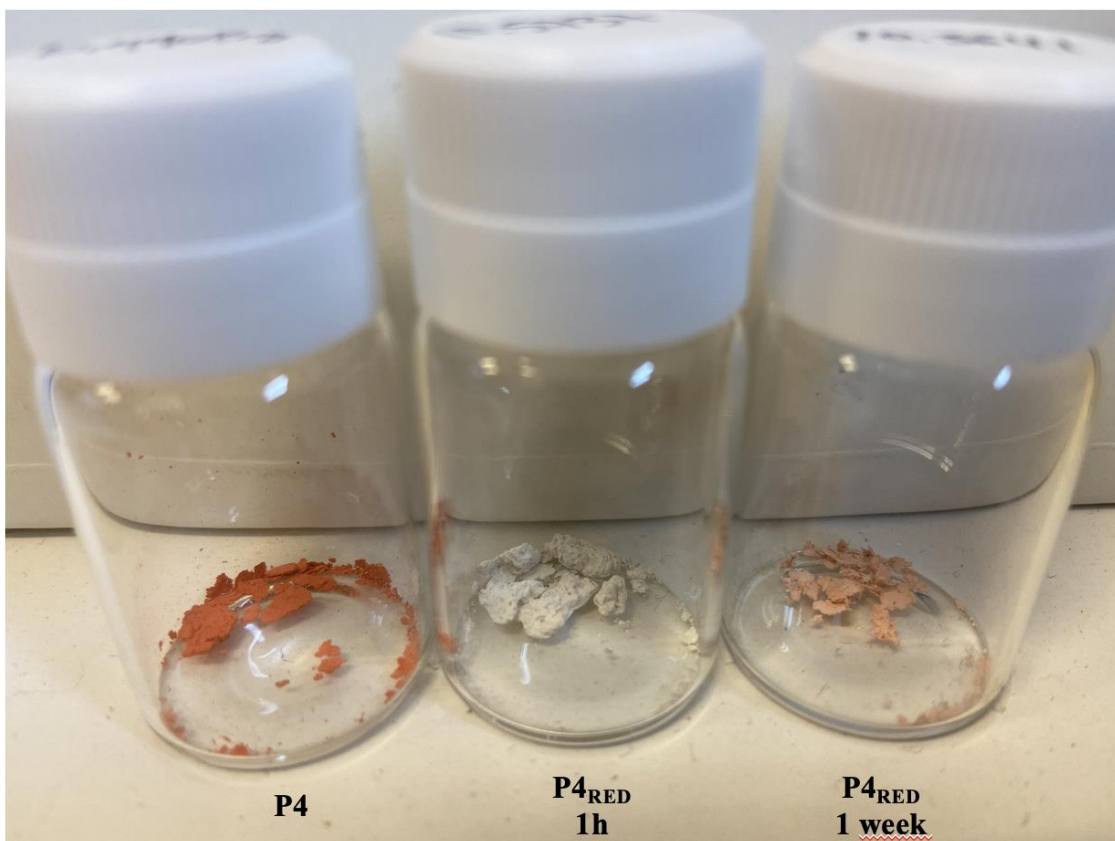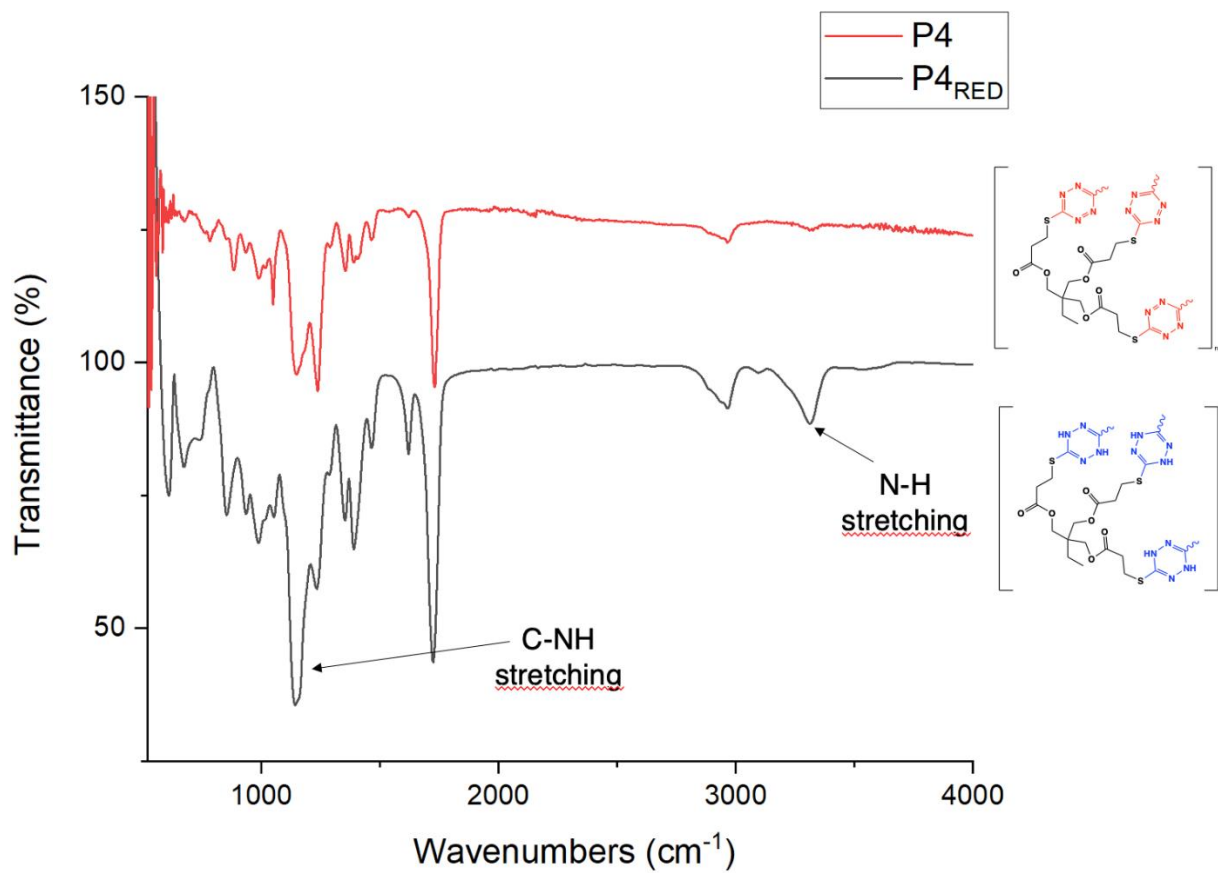*Image of P1, P1_RED after 1h and P1_RED after 1 week.*

P4_{RED}

*P4*_{RED}

| P4 | | P4_{RED} |
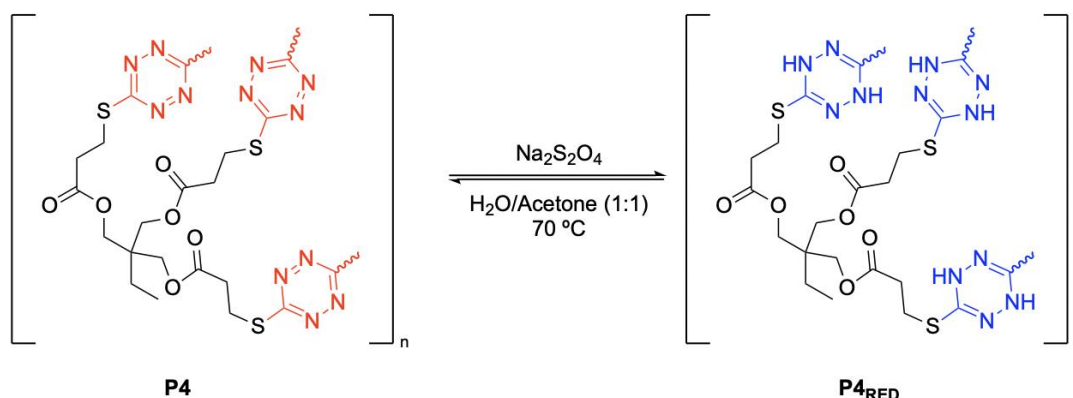
P4 (80 mg, 1 eq) and sodium dithionite (607.8 mg, 20 eq) were placed in a round bottom flask and refluxed for 48 h in a 1:1 acetone/water mixture (17.5 mL, 0.01 M). The solution was cooled to room temperature and the obtained white solid was filtered and washed with ACN (2 x 20 mL), Milli-Q H_2O (2 x 20 mL), MeOH (2 x 20 mL) and vacuum dried for 5 min. Finally, the polymer was dried on a high vacuum pump for 3-4 h. 65 mg, 80 % yield.

NOTE: This polymer slowly reoxidizes by air contact. The reduction was confirmed by IR.

IR analysis:

The reduction reaction exposed a similar spectrum for **P4**_{RED} and **P4**, except the characteristic peaks for the N-H stretching of the reduced tetrazine around 3350 cm^{-1} and the new C-N stretching near 1200 cm^{-1}.

N-H
stretching

C-NH
stretching

Image of P4, P4$_{RED}$ after 1h and P4$_{RED}$ after 1 week.
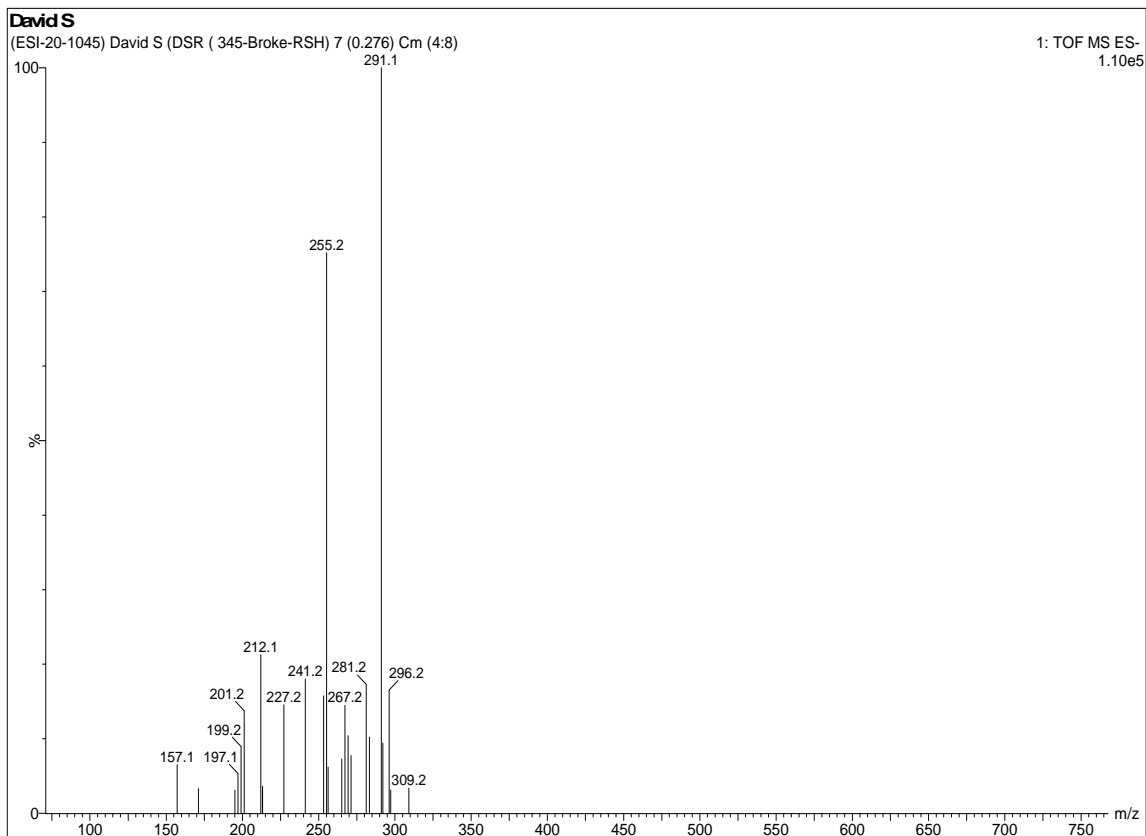
5. Degradation experiments

Degradation of P1 with dodecanthiol
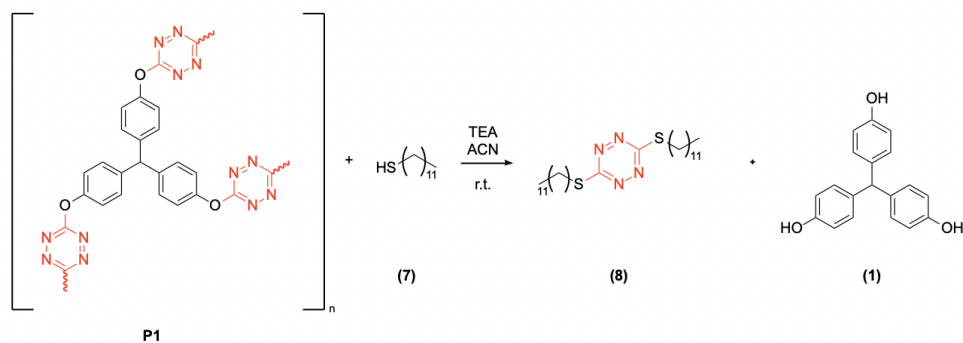
P1 (11.5 mg, 1 eq) was suspended in CD_3CN (1 mL) and dodecanthiol (0.04 mL, 6 eq) was added followed by TEA (0.03 mL, 6 eq) and the reaction was stirred a room temperature O.N. After the complete disappearance of the polymer, the process was monitored by ^1H-NMR and mass spectroscopy.
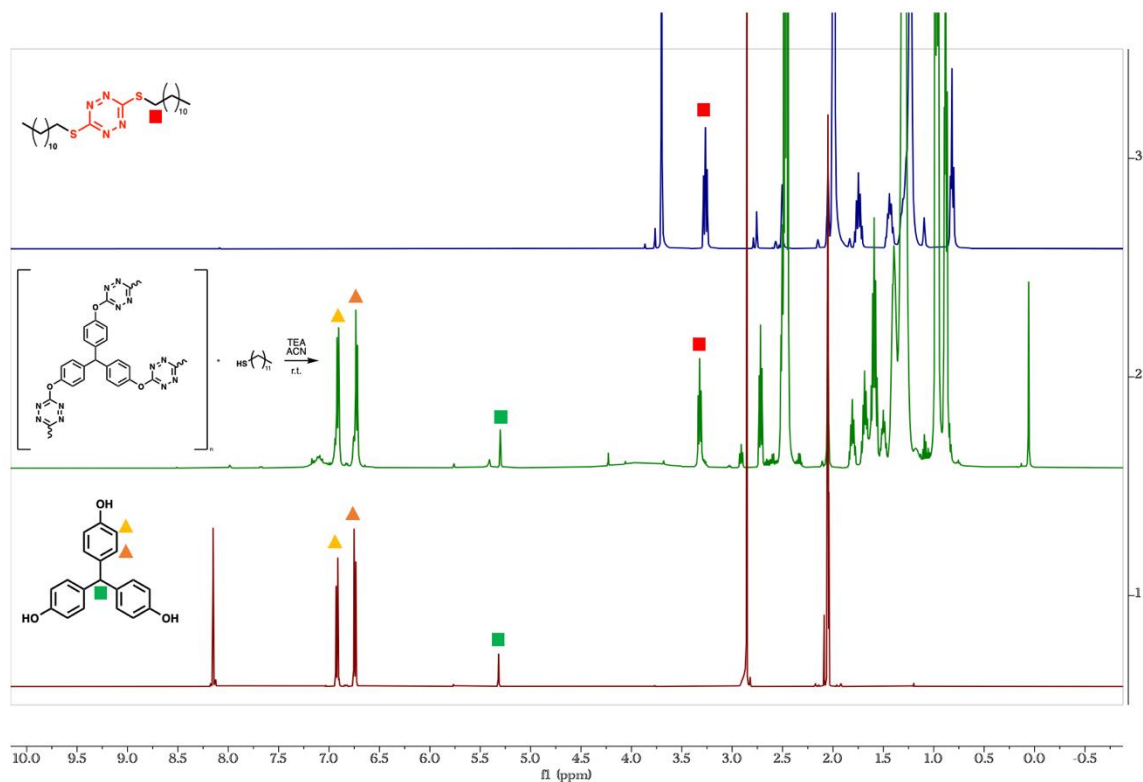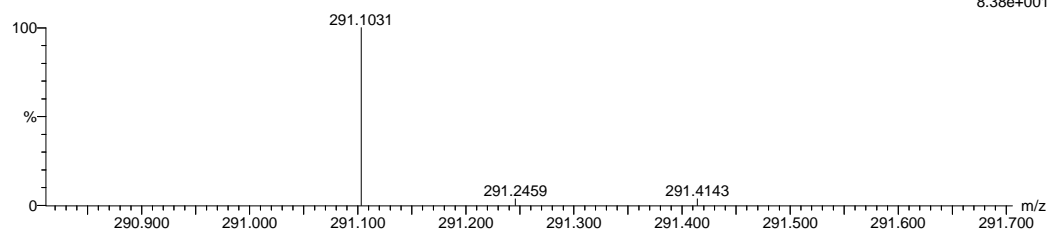

Degradation of P1.

HRMS spectra of P1 degradation.

Elemental Composition Report   **Page 1**

Tolerance = 5.0 PPM   /   DBE: min = -3.0, max = 120.0
Element prediction: Off
Number of isotope peaks used for i-FIT = 3

Monoisotopic Mass, Even Electron Ions
429 formula(e) evaluated with 3 results within limits (all results (up to 1000) for each mass)
Elements Used:
C: 0-60   H: 0-75   N: 0-3   O: 0-10   Na: 0-2

Minimum:	20.00				-3.0			
Maximum:	100.00		5.0	5.0	120.0			
Mass	RA	Calc. Mass	mDa	PPM	DBE	i-FIT	i-FIT (Norm)	Formula
291.1031	100.00	291.1032	-0.1	-0.3	-2.5	22.5	0.8	C8 H21 O8 Na2
		291.1040	-0.9	-3.1	-0.5	22.4	0.7	C7 H19 N2 O10
		291.1021	1.0	3.4	12.5	24.4	2.8	C19 H15 O3

HRMS data of P1 degradation.

32

### Degradation Kinetics:

P1 (7.2 mg, 1 eq) was placed in an NMR tube. Solutions in acetone-D_6 of dodecanthiol (6 eq), TEA (6 eq) and hexamethyldisilane (1.1 eq) as internal standard, were added reaching a final volume of 0.6 mL. The reaction was sonicated in intervals of 30 min and monitored by ^{1}H-NMR. The final concentration of the phenol **1** (0.029 mM) accounts for a 99% of recovery.
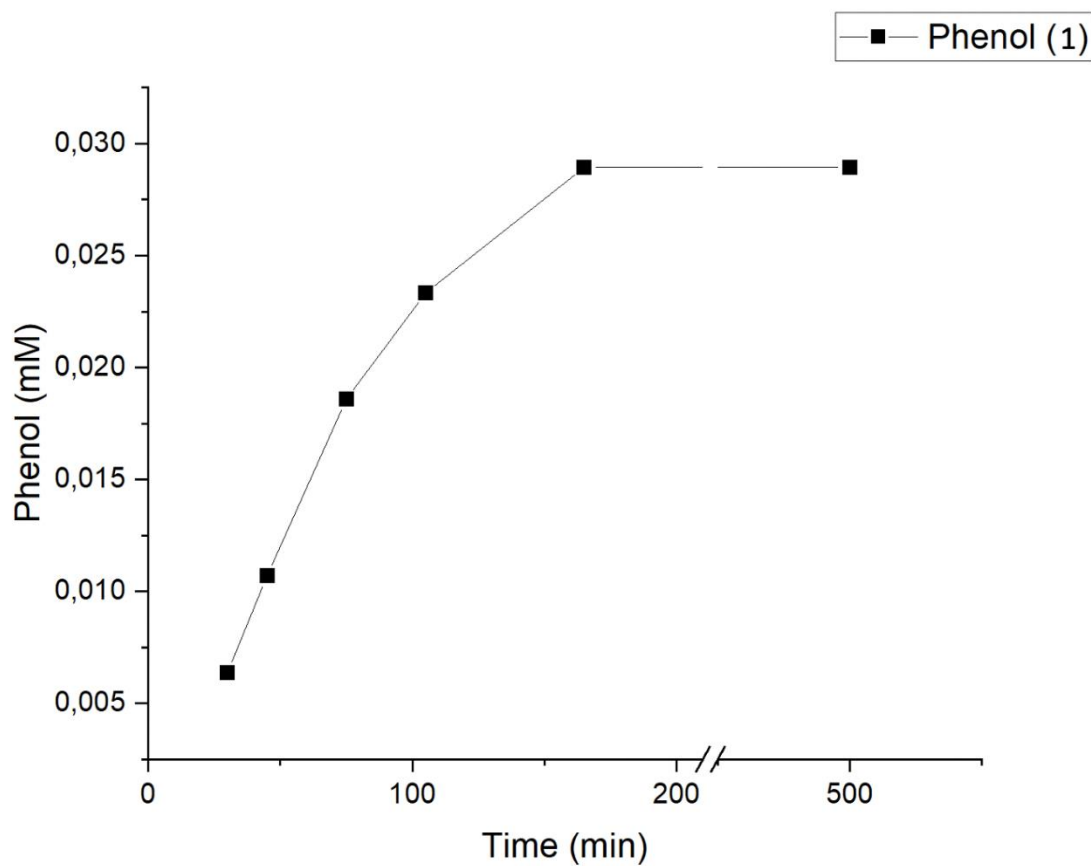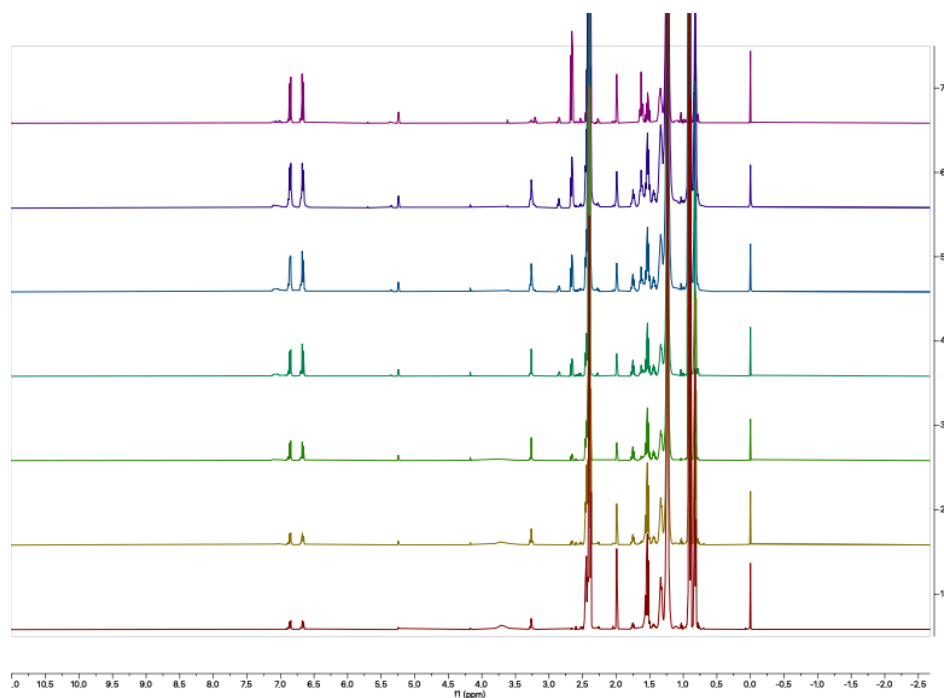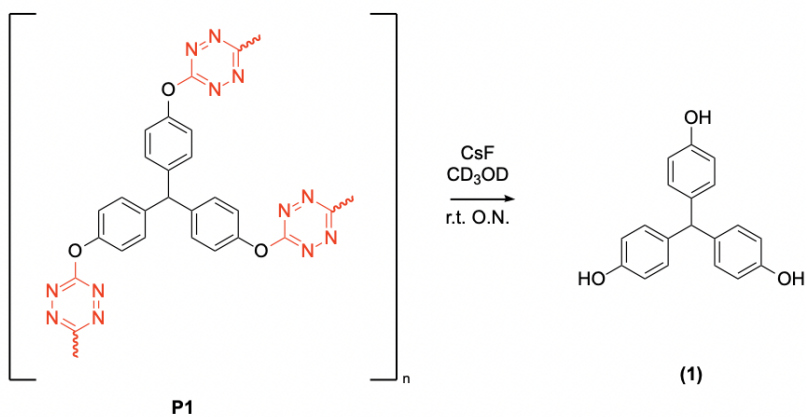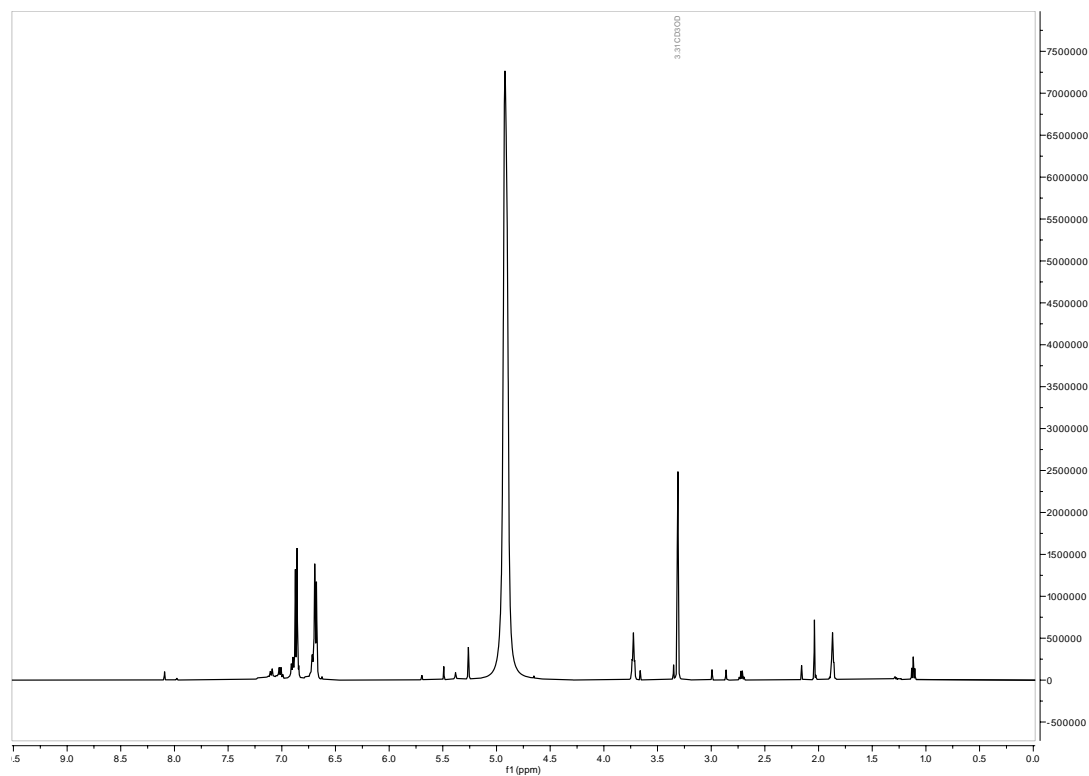
P1 degradation experiment ^{1}H-NMR stack plot.
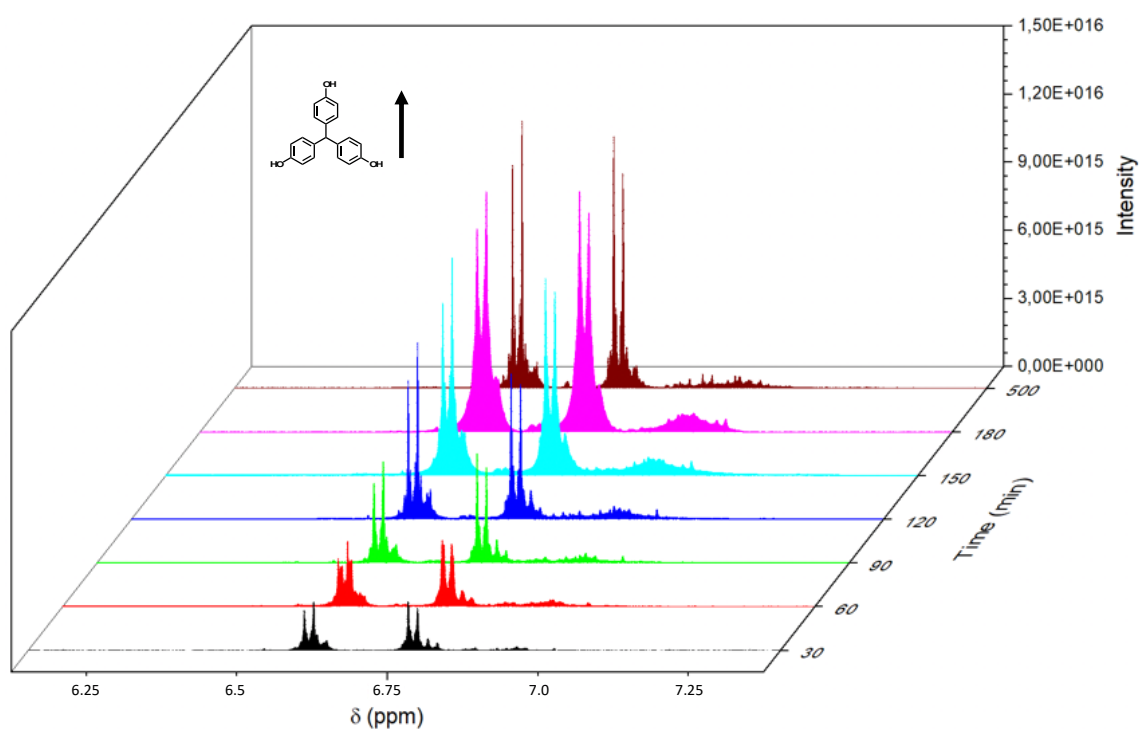
P1 degradation experiment ^{1}H-NMR 3D-stack plot.
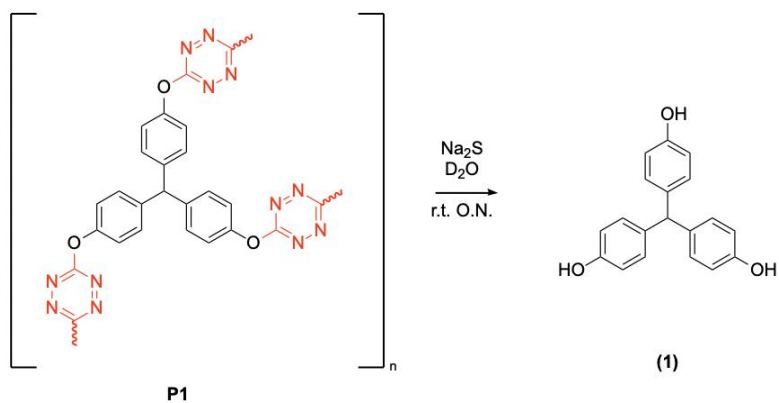
Degradation of P1with CsF.

P1

(1)

P1 (10.0 mg, 1 eq) was suspended in CD$_3$OD (1 mL), CsF (6 eq) was added. The reaction was stirred a room temperature O.N. After the complete disappearance of the polymer, the process was monitored by ^{1}H-NMR.
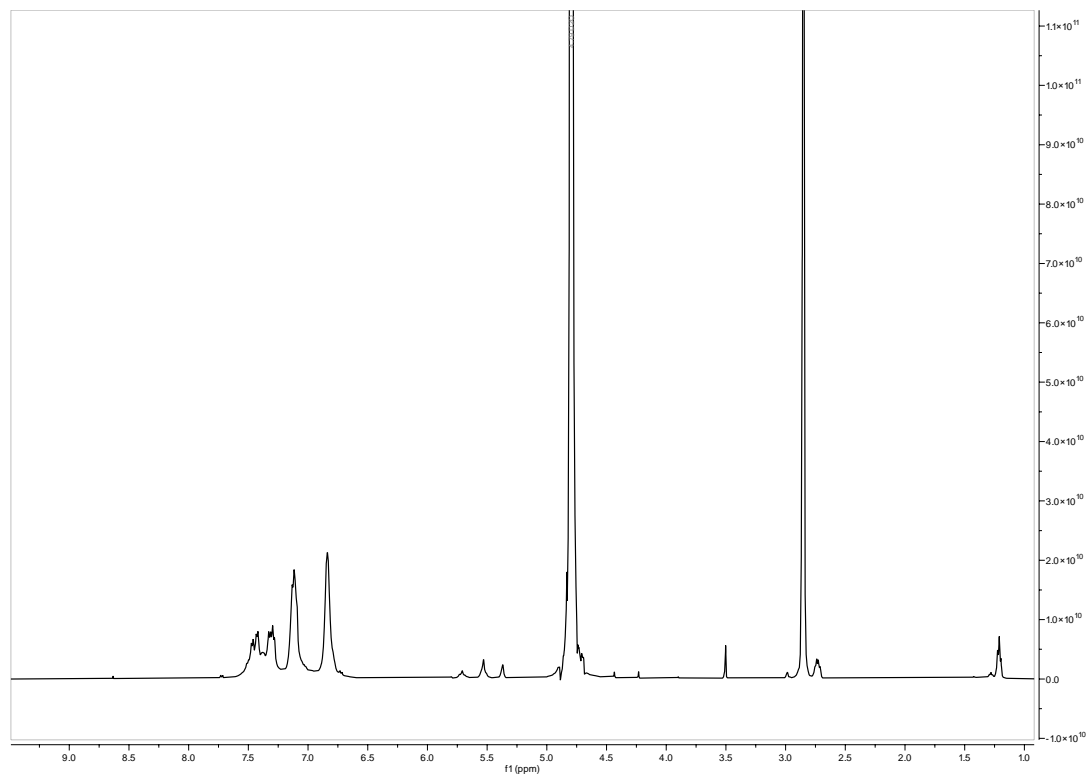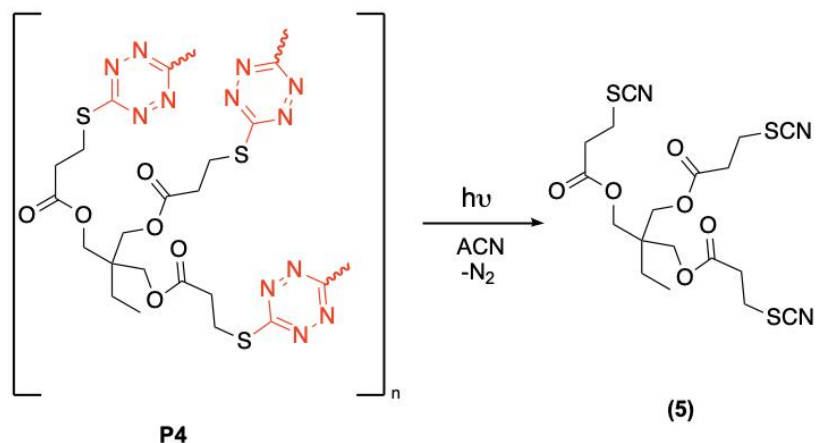
Degradation of P1 with Hydrogen Sulfide.

P1 (11.2 mg, 1 eq) was suspended in D_2O (1 mL) and $Na_2S·5H_2O$ (4 eq) was added. The reaction was stirred a room temperature O.N. After the complete disappearance of the polymer, the process was monitored by ^{1}H-NMR.
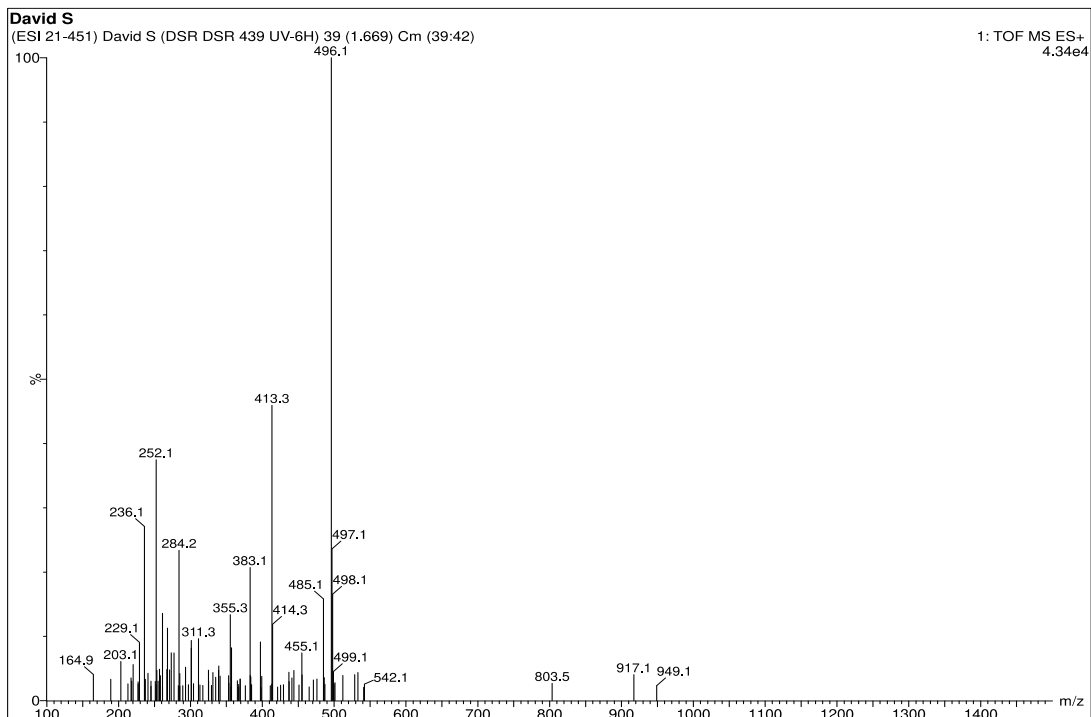
Degradation of P4 by light.

P4

(5)

P4 (7.0 mg) was suspended in CD₃CN (1 mL) in a UV glass cuvette, and it was irradiated with an ACE-Hanovia photochemical lamp 7830-60 (450W) while stirring. The process was monitored by ^{1}H-NMR until the complete disappearance of the red solid and confirmed by HRMS.

(ESI 21-451) David S (DSR DSR 439 UV-6H) 39 (1.669) Cm (39:42)

1: TOF MS ES+
4.34e4
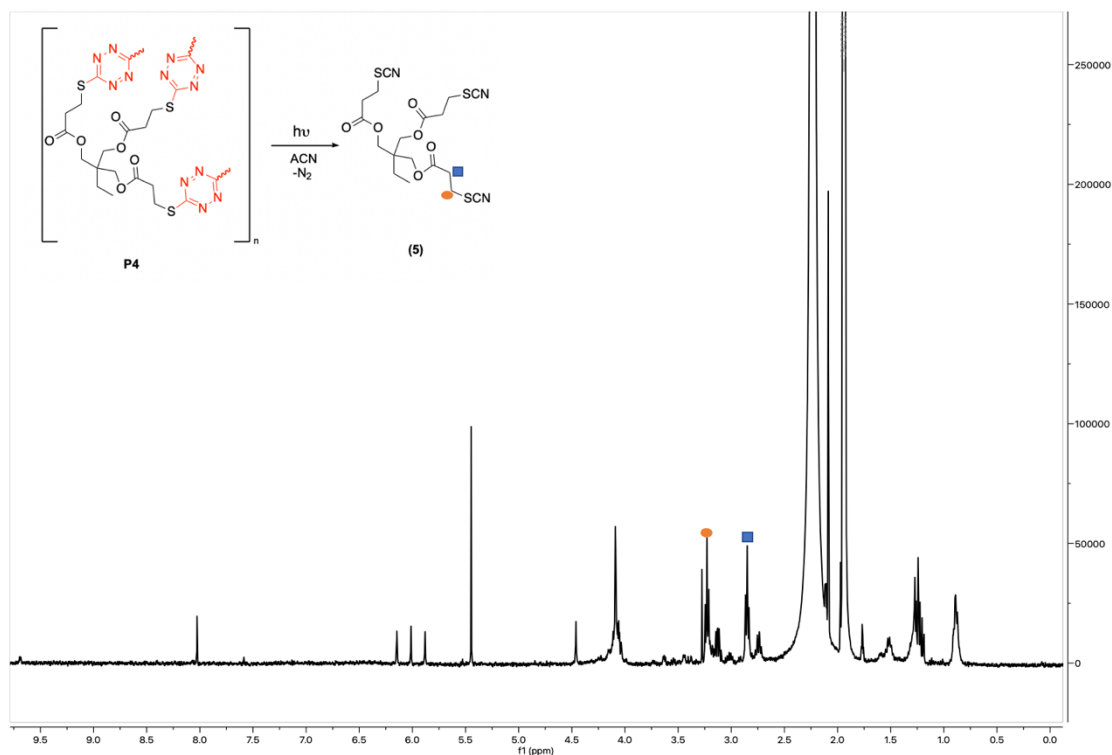
Elemental Composition Report

Multiple Mass Analysis: 3 mass(es) processed
Tolerance = 5.0 PPM   /   DBE: min = -1.5, max = 100.0
Element prediction: Off
Number of isotope peaks used for i-FIT = 3

Monoisotopic Mass, Even Electron Ions
1023 formula(e) evaluated with 2 results within limits (up to 50 best isotopic matches for each mass)
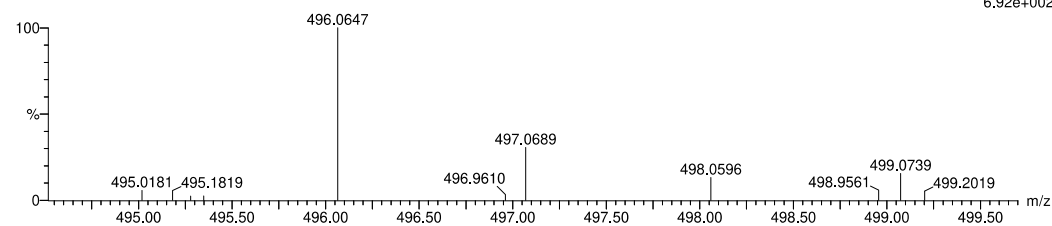Elements Used:
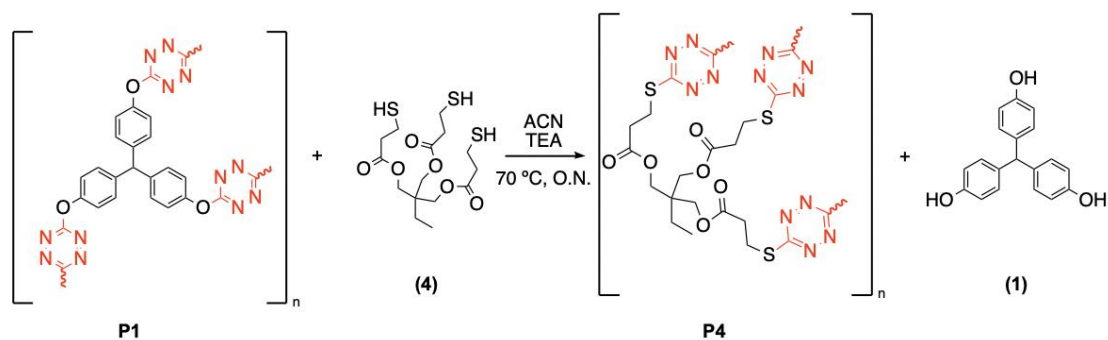C: 0-19   H: 0-23   N: 0-3   O: 0-10   Na: 0-1   S: 0-3
David S
(ESI 21-451) David S (DSR DSR 439 UV-6H) 38 (1.270)

2: TOF MS ES+
6.92e+002

| Minimum: | 15.00 | | | | -1.5 | | | |
| Maximum: | 100.00 | | 5.0 | 5.0 | 100.0 | | | |

Mass	RA	Calc. Mass	mDa	PPM	DBE	i-FIT	i-FIT (Norm)	Formula
496.0647	100.00	496.0647	0.0	0.0	8.5	16.7	0.0	C18 H23 N3 O6 Na S3
497.0689	30.52	497.0664	2.5	5.0	8.5	32.5	0.0	C18 H22 N2 O9 Na S2
499.0739	15.51	---						

6. Metamorphosis experiments

P1 (100 mg, 1 eq) was suspended in ACN (25 mL, 0.01 M). Thiol **4** (1 eq) was added followed by TEA (2 eq) and the solution was stirred O.N. at 70 °C. The reaction was allowed to cool, and the polymer was filtered, washed with ACN (2 x 20 mL), Milli-Q H_2O (2 x 20 mL), MeOH (2 x 20 mL) and vacuum dried for 5 min. Finally, the polymer was dried on a high vacuum pump for 3-4 h. Anal. Calc. for $(C_{18}H_{23}N_6O_6S_3)\cdot(MeOH)_{0.25}\cdot(ACN)_{0.05}$: C, 41.93; H, 4.50; N, 16.30; O, 18.62; S, 18.65. Found: C, 48.10; H, 5.09; N, 12.07; O, 19.56; S, 15.19. The slight differences in the elemental analysis could be due to little defects on the metamorphosis process.
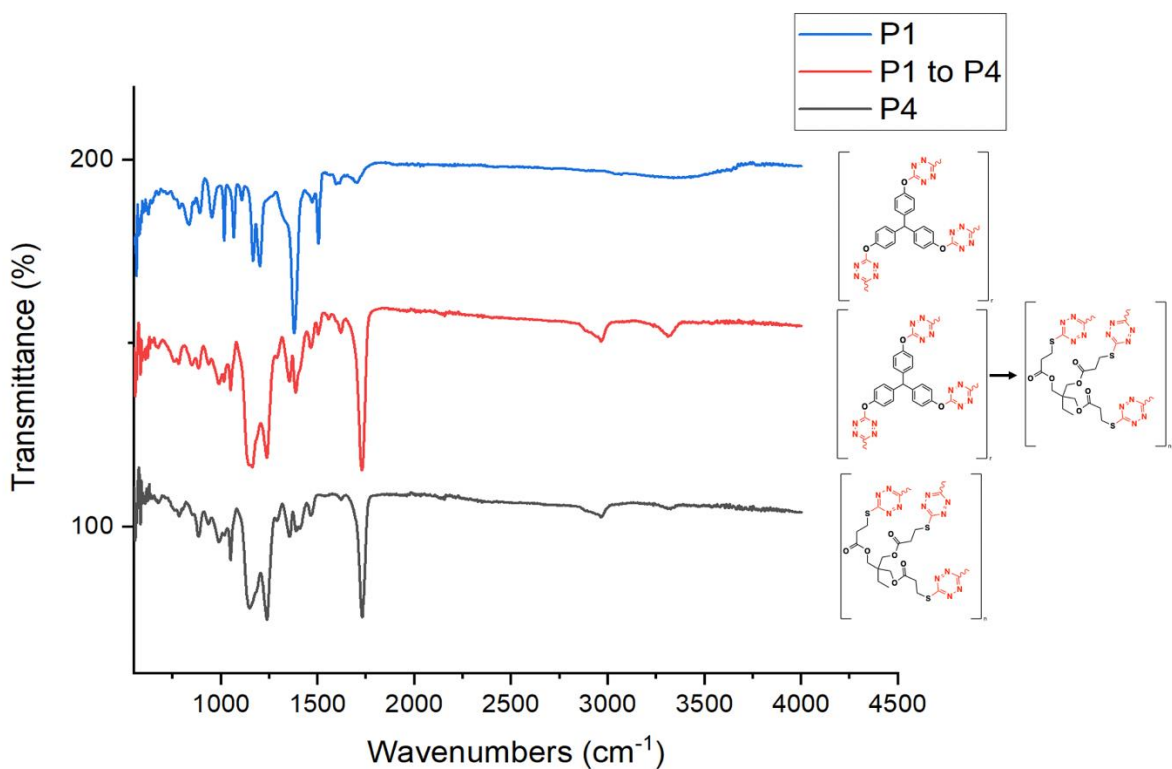
NOTE: This procedure was repeated in CD_3CN, and the release of phenol **1** was monitored by ^1H-NMR of the liquid phase.
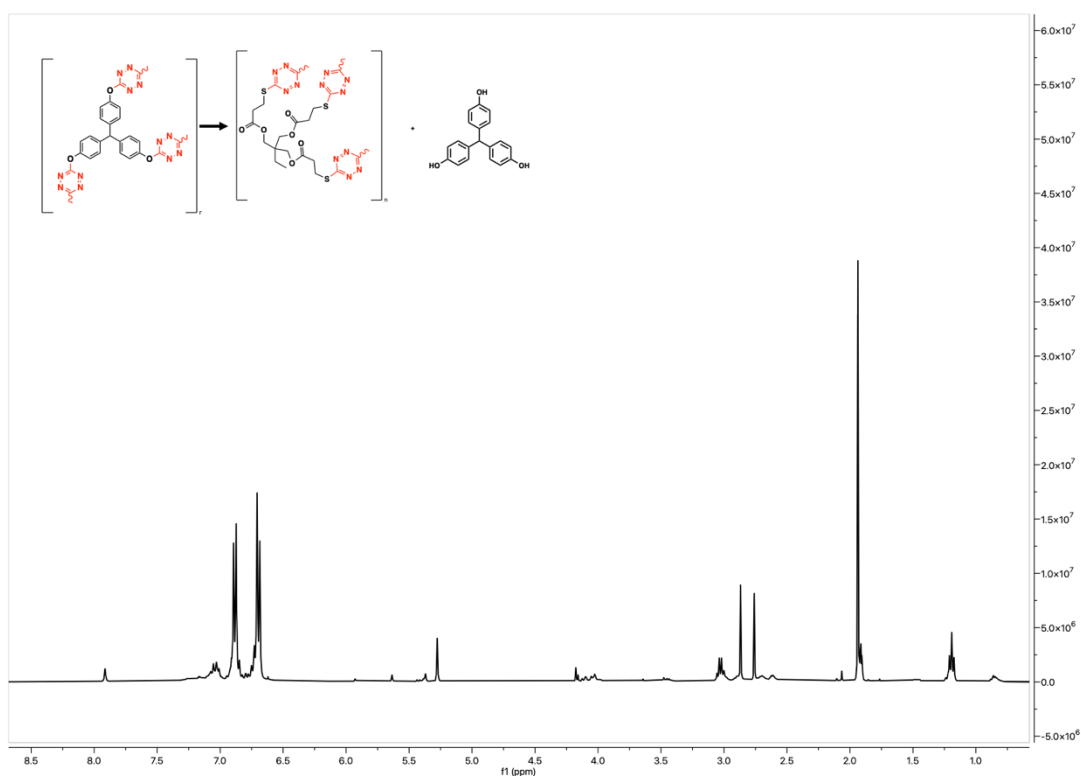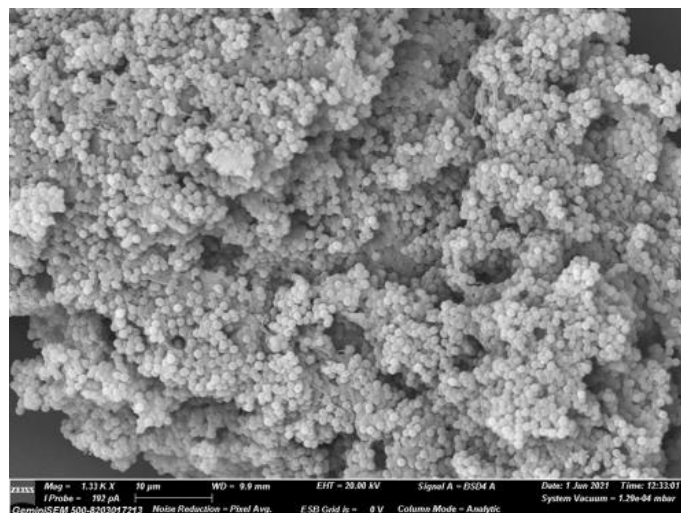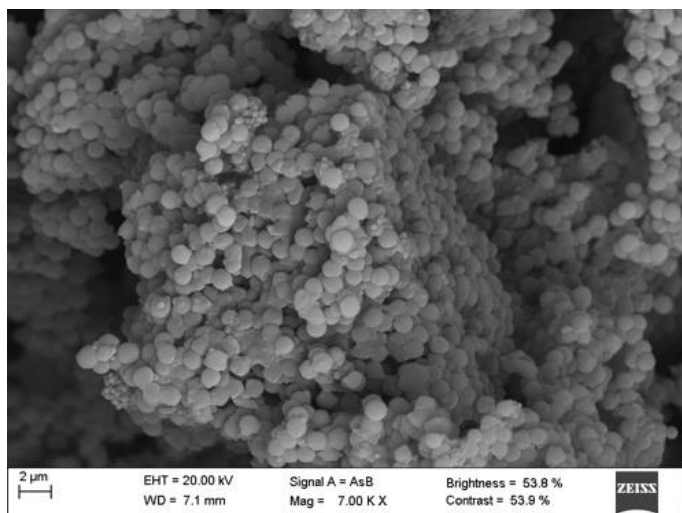

NMR of liquid phase in Metamorphosis reaction.

IR analysis:

The metamorphosis experiment gave the same IR spectra for the product obtained from the reaction (red) than P4 (black).

SEM images:

7. <u>References</u>

(1)   T. Santos, D. S. Rivero, Y. Pérez-Pérez, E. Martín-Encinas, J. Pasán, A. H. Daranas, R. Carrillo, Dynamic Nucleophilic Aromatic Substitution of Tetrazines. *Angew. Chemie Int. Ed.* **2021**, *60*, 18783-18791. https://doi.org/10.1002/anie.202106230

(2)   S. Zhao, X. Huang, A. J. Whelton, M. M. Abu-Omar, Renewable Epoxy Thermosets from Fully Lignin-Derived Triphenols. *ACS Sustain. Chem. Eng.* **2018**, *6* (6), 7600–7608. https://doi.org/10.1021/acssuschemeng.8b00443.